INTERNATIONAL JOURNAL OF
NUMERICAL ANALYSIS AND MODELING
Volume 11, Number 3, Pages 541–566

HIGHER DEGREE IMMERSED FINITE ELEMENT METHODS FOR SECOND-ORDER ELLIPTIC INTERFACE PROBLEMS

SLIMANE ADJERID, MOHAMED BEN-ROMDHANE, AND TAO LIN

Abstract. We present higher degree immersed finite element (IFE) spaces that can be used to solve two dimensional second order elliptic interface problems without requiring the mesh to be aligned with the material interfaces. The interpolation errors in the proposed piecewise p^{th} degree spaces yield optimal $\mathcal{O}(h^{p+1})$ and $\mathcal{O}(h^p)$ convergence rates in the L^2 and broken H^1 norms, respectively, under mesh refinement. A partially penalized method is developed which also converges optimally with the proposed higher degree IFE spaces. While this penalty is not needed when either linear or bilinear IFE space is used, a numerical example is presented to show that it is necessary when a higher degree IFE space is used.

Key words. Immersed finite element, immersed interface, interface problems, Cartesian mesh method, structured mesh, higher degree finite element

1. Introduction

Mathematical modeling of a physical phenomenon in a domain consisting of multiple materials often leads to an interface problem whose exact solution is required to satisfy jump conditions across the material interfaces in addition to the pertinent partial differential equation and the related boundary conditions. Conventional finite element methods with body-fitted meshes can be used to solve interface problems with standard problem independent finite element basis functions. In general, to achieve the optimal convergence of conventional finite element solutions, elements which are cut by the interface should be avoided [6, 9, 12]. This restriction leads to several drawbacks, among which are

(i) The need for remeshing, sometimes many times, when solving problems with moving interfaces. The same difficulty occurs for random interfaces where many problems are solved with different interfaces (from different values of the parameters) to estimate quantities of interest such as the expected solution.
(ii) Excessive mesh refinement to resolve small structures such as thin layers in the domain.
(iii) Prohibition of the use of uniform meshes when solving problems whose interfaces have nontrivial geometries.

In the 1970s and 1980s, Babuška et al. [4, 5] developed the generalized finite element method using the idea of constructing the basis functions on an element by locally solving the interface problem in that element. Instead of generic polynomials, they developed problem dependent local basis functions which may be non-polynomials and are capable of capturing important features of the exact solution. The recently developed IFE methods [2, 3, 11, 14, 15, 18, 19, 20, 21, 22]

Received by the editors June 2, 2013 and, in revised form, March 6, 2014.
2000 *Mathematics Subject Classification.* 65N15, 65N30, 65N50, 35R05.
This research was partially supported by the National Science Foundation (Grant Number DMS 1016313) .

extended this idea and used the jump conditions in the interface problem to construct local basis functions with piecewise polynomials. This idea is similar to Hsieh-Clough-Tocher macro elements [8, 13] in which piecewise cubic polynomials on three sub-triangles are used to satisfy the required continuity. IFE methods use meshes that can be independent of interface geometry; hence they can circumvent the limitations mentioned above for conventional finite element methods.

We note that almost all IFE spaces proposed up to now are based on linear, bilinear, or trilinear polynomials [20, 21, 22, 28] except for those constructed for one dimensional interface problems [2, 3, 11]. It is of great interests to develop higher degree IFE spaces to be used in more efficient schemes such as those based on discontinuous Galerkin formulations with local h and p refinement capabilities. In this manuscript, we present procedures to construct arbitrarily higher degree IFE spaces for solving the typical second order elliptic interface problem on a triangular Cartesian mesh.

Following the usual IFE framework, we use standard finite element shape functions on non-interface elements and we focus on how to construct higher degree IFE shape functions in interface elements with piecewise polynomials that satisfy the interface jump conditions required by an interface problem. However, as first observed in [11], extra constraints need to be carefully introduced in order to uniquely determine higher degree IFE functions with the optimal approximation capability according to the degree of polynomials employed. Based on the idea in [2, 3], we propose to construct higher degree IFE spaces with the interface jump conditions required by the second order elliptic interface problem plus one of the two classes of extended interface jump conditions. Both classes of extended jump conditions involve higher order derivatives. In the first class, the second-order elliptic operator and its normal derivatives of a higher degree IFE function are required to be continuous across the interface. The second class of extended jump conditions enforce the continuity of higher order normal derivatives of the flux of an IFE function.

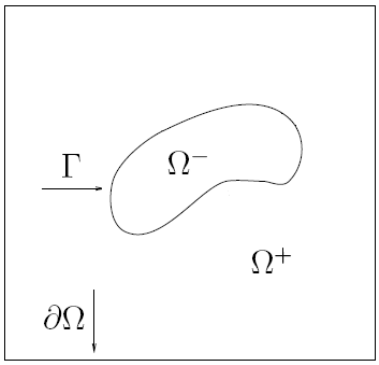

FIGURE 1.1. A two-material domain Ω

IFE functions are generally not continuous across interface edges; hence IFE methods for interface problems are usually nonconforming in the sense that these IFE spaces are not subspaces of $H^1(\Omega)$ to which the exact solution belongs. While a simple Galerkin formulation works satisfactorily for both the linear and bilinear IFE spaces [15, 18, 20, 22], we have noticed that the discontinuity of higher degree IFE functions across interface edges cannot be neglected in developing numerical schemes for solving interface problems. We have found that penalization

techniques used in discontinuous Galerkin methods work well with higher degree IFE space presented here. The penalization can be employed over interface edges only to augment the simple Galerkin formulation or it can be used in a discontinuous Galerkin formulation through all edges of a mesh. The proposed p^{th} degree IFE spaces combined with a partially penalized finite element formulation are able to optimally resolve the non-smooth behavior of the solution across the interface without requiring the mesh to be aligned with the material discontinuity.

To be specific, we consider a bounded open set $\Omega \subset \mathbb{R}^2$ that is separated into two subsets Ω^+ and Ω^- by a curve Γ, see Figure 1.1. In this domain, we consider the following typical two dimensional second order elliptic interface problem

$$\begin{cases} -\nabla \cdot (\beta \nabla u) = f, & \text{on } \Omega, \\ u_{|\partial\Omega} = g, \end{cases} \tag{1.1a}$$

whose true solution u and its normal flux are required to be continuous across the interface Γ as

$$[u]_\Gamma = 0, \tag{1.2a}$$

and

$$[\beta \frac{\partial u}{\partial \boldsymbol{n}}]_\Gamma = 0, \tag{1.2b}$$

where $[v]_\Gamma = v^+|_\Gamma - v^-|_\Gamma$ denotes the jump of a function v across the interface Γ. Here $v^\pm = v|_{\Omega^\pm}$ and $\frac{\partial v}{\partial \boldsymbol{n}} = \boldsymbol{n} \cdot \nabla v$ denotes the normal derivative of v on the interface Γ with $\boldsymbol{n}$ being a unit normal vector to Γ. The material coefficient β is assumed to be piecewise constant in the following form

$$\beta(X) = \begin{cases} \beta^-, & \text{when } X \in \Omega^-, \\ \beta^+, & \text{when } X \in \Omega^+. \end{cases} \tag{1.3}$$

In this exploratory research stage, we focus on problems with a linear interface Γ defined by the equation

$$y = Ax + B. \tag{1.4}$$

Our choice here is mainly based on two reasons. *(I)*. There are many important applications with linear interfaces such as uniform coating and layered materials; *(II)*. We believe that our explorations here can shed light on how to handle general curve interfaces in the next step of research.

This manuscript is organized as follows. In Section 2, we discuss how to set up suitable extended jump conditions that can be used to construct quadratic IFE spaces. We further show that these IFE spaces exist and determine their dimension. We also propose hierarchical IFE shape functions that could be used to efficiently implement p-enrichment for IFE methods. In Section 3 we describe a framework for constructing general higher degree IFE spaces. In Section 4 we introduce a higher degree IFE method with penalties partially imposed over interface edges. In Section 5 we present numerical experiments to demonstrate the optimal approximation capability of the proposed higher degree IFE spaces, and we conclude with a few remarks in Section 6.

2. Quadratic IFE spaces

In this section we show how to construct quadratic IFE spaces for the two dimensional second order elliptic interface problem and prove their existence and uniqueness. We further establish several properties of the proposed IFE spaces and

construct their Lagrange and hierarchical IFE shape functions. From now on, we use $\mathcal{P}_k$ to denote the space of two-dimensional polynomials of degree k:

$$\mathcal{P}_k = \{p|\ p(\xi,\eta) = \sum_{l=0}^{k}\sum_{i=0}^{l} c_i^l \xi^i \eta^{l-i}\}. \tag{2.1}$$

2.1. Jump conditions for quadratic IFE spaces. Let $\mathcal{T}_h$ be a regular triangular mesh of size h for the domain Ω, where h is the maximum diameter. The set of interface elements that are cut by the interface is denoted by $\mathcal{T}_h^i$. Similarly, edges that are cut by the interface are called interface edges; otherwise, they are referred to as non-interface elements or edges. As illustrated in Figure 2.1, every interface element $T = \triangle V_1V_2V_3$ can be split as

$$T = T^+ \cup T^-,\ \text{where}\ \ T^{\pm} = T \cap \Omega^{\pm}. \tag{2.2}$$

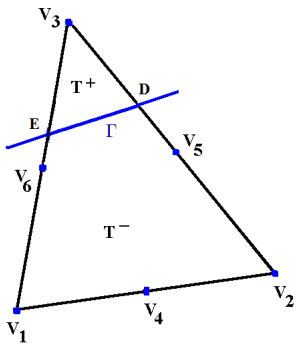

FIGURE 2.1. A physical interface element

In the discussion from now on, we will use V_4, V_5 and V_6 to denote the midpoints of the edges of a triangular element T such that

$$V_4 = \frac{1}{2}(V_1+V_2),\ V_5 = \frac{1}{2}(V_2+V_3),\ V_6 = \frac{1}{2}(V_3+V_1).$$

First we introduce the following quadratic IFE spaces on an arbitrary interface element T

$$\mathcal{R}_1^2(T) = \{U\ |\, U|_{T^{\pm}} \in \mathcal{P}_2,\ [U]_{T\cap\Gamma} = [\beta\frac{\partial U}{\partial \boldsymbol{n}}]_{T\cap\Gamma} = [\beta\Delta U]_{T\cap\Gamma} = 0\}, \tag{2.3a}$$

$$\mathcal{R}_2^2(T) = \{U\ |\, U|_{T^{\pm}} \in \mathcal{P}_2,\ [U]_{T\cap\Gamma} = [\beta\frac{\partial U}{\partial \boldsymbol{n}}]_{T\cap\Gamma} = [\beta\frac{\partial^2 U}{\partial \boldsymbol{n}^2}]_{T\cap\Gamma} = 0\}. \tag{2.3b}$$

These local IFE spaces can be used to construct global IFE spaces over the whole domain Ω. The motivations for us to consider these IFE spaces are as follows.

On an interface triangle T, let $\varphi(x,y)$ be a piecewise quadratic function written as

$$\varphi(x,y) = \begin{cases} \varphi^+(x,y)\,, & \text{on}\ \ T^+ \\ \varphi^-(x,y)\,, & \text{on}\ \ T^-, \end{cases} \tag{2.4}$$

where $\varphi^{\pm}(x,y) \in \mathcal{P}_2$. Thus, φ is determined by 12 independent parameters. A piecewise quadratic function $\varphi \in \mathcal{R}_1^2(T)$ satisfies

$$[\varphi]_{\Gamma} = 0, \tag{2.5a}$$

$$[\beta\ \boldsymbol{n}\cdot\nabla\varphi]_\Gamma = 0, \tag{2.5b}$$

$$[\beta\Delta\varphi]_\Gamma = 0. \tag{2.5c}$$

The two conditions (2.5a) and (2.5b) follow from the physical jump conditions (1.2a) and (1.2b); however, the jump equation (2.5c) is suggested by the continuity of the function f on the right-hand side in (1.1a).

Guided by our work of the one-dimensional IFE methods in [2, 11] we can also construct piecewise quadratic functions that satisfy, instead of (2.5c), the following weaker condition for the second normal derivative

$$[\beta\frac{\partial^2\varphi}{\partial\boldsymbol{n}^2}]_\Gamma = 0, \tag{2.6}$$

which leads to the piecewise quadratic polynomial space $\mathcal{R}_2^2(T)$.

Since interface jump conditions (2.5c) and (2.6) are not in the original interface problem, we refer to them as the extended interface jump conditions. These extended jump conditions are needed to uniquely determine the quadratic IFE functions in $\mathcal{R}_k^2(T),\ k=1,2$ on each interface element $T\in\mathcal{T}_h$ and to guarantee the desired optimal approximation capability.

We now describe how to use the reference triangle $\hat{T}=\triangle\hat{V}_1\hat{V}_2\hat{V}_3$ to define the functions in $\mathcal{R}_k^2(T),\ k=1,2$, where $\hat{V}_1=(0,0)^t$, $\hat{V}_2=(1,0)^t$ and $\hat{V}_3=(0,1)^t$. Without loss of generality, we assume that the vertices of each interface element $T=\triangle V_1V_2V_3\in\mathcal{T}_h$ are arranged such that the vertex shared by the two interface edges is V_3. We consider each element $T=\triangle V_1V_2V_3\in\mathcal{T}_h$ with $V_i=(x_i,y_i)^T$ as the image of $\hat{T}$ through the affine mapping $F^{-1}:\hat{T}\to T$ defined as

$$\begin{pmatrix}x\\y\end{pmatrix} = F^{-1}(\hat{x},\hat{y}) = V_1+(V_2-V_1)\hat{x}+(V_3-V_1)\hat{y}, \tag{2.7a}$$

where $F:T\to\hat{T}$ can be written as

$$F(x,y)=\mathbf{J}\begin{pmatrix}x\\y\end{pmatrix}-\mathbf{J}\ V_1=\begin{pmatrix}\hat{x}\\\hat{y}\end{pmatrix},\quad \mathbf{J}=\begin{pmatrix}x_2-x_1 & x_3-x_1\\ y_2-y_1 & y_3-y_1\end{pmatrix}^{-1}. \tag{2.7b}$$

As usual, with a function $\hat{\varphi}$ defined on $\hat{T}$, we define a corresponding function on T as follows

$$\varphi(x,y)=\hat{\varphi}(\hat{x},\hat{y})=\hat{\varphi}(F(x,y)). \tag{2.7c}$$

Since the interface is linear, it intersects two edges of every interface triangle creating 12 possible cases as shown in Figure 2.2. Furthermore, interface elements can be grouped into three types. Elements of Type I are shown in the first column with one vertex on one side of the interface and the remaining five nodes on the other side; elements of Type II are shown in the second column where two nodes are on one side and the remaining four nodes are on the other side, and elements of Type III are in the third column where the six nodes are equally distributed on both sides of the interface. All interface elements of a given type are mapped to the corresponding reference interface triangle shown in the first row of Figure 2.2.

For each type of reference triangles, we refer to the sub-domain of $\hat{T}$ containing vertex $\hat{V}_3$ as $\hat{T}^1$ and let $\hat{T}^2=\hat{T}\setminus\hat{T}^1$. The discontinuous material coefficient $\hat{\beta}$ on the reference interface triangle $\hat{T}$ is accordingly written as

$$\hat{\beta}=\begin{cases}\hat{\beta}^1, & \text{on } \hat{T}^1,\\ \hat{\beta}^2, & \text{on } \hat{T}^2,\end{cases} \tag{2.8}$$

where $\hat{\beta}^i=\beta^\pm$ if $\hat{T}^i=F(T^\pm)$.

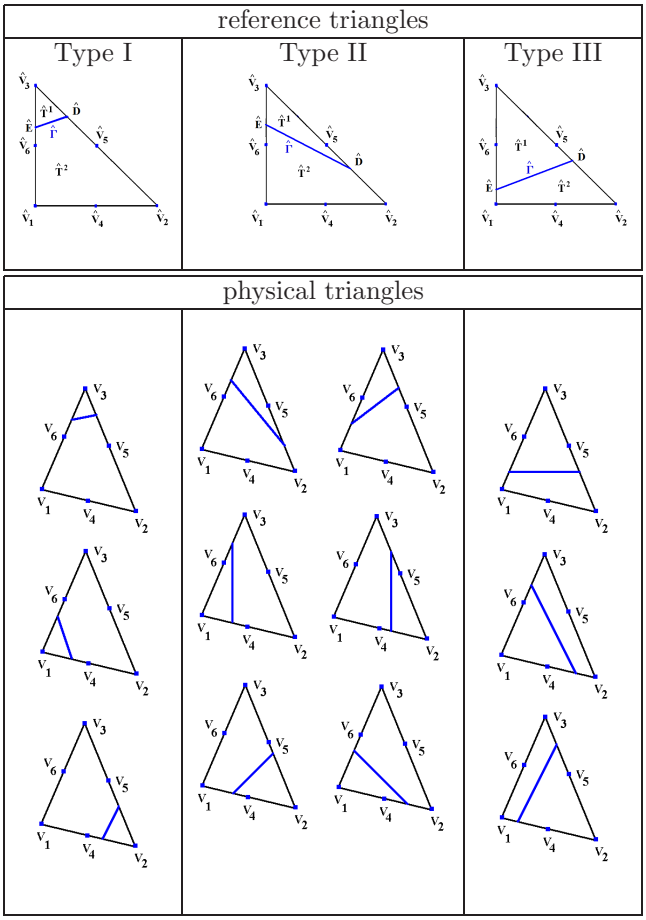

FIGURE 2.2. Interface elements of Type I and corresponding reference triangle (1^{st} column), elements of Type II and corresponding reference triangle (2^{nd} column) and elements of Type III and corresponding reference triangle (3^{th} column).

In order to construct piecewise quadratic functions on the reference triangles, we need to map the jump conditions to the reference triangles. First, we apply the interface jump conditions to the piecewise quadratic function $\hat{\varphi}$ on $\hat{\Gamma} = F(\Gamma \cap T)$:

$$[\hat{\varphi}]_{\hat{\Gamma}} = 0, \tag{2.9a}$$

$$[\hat{\beta}\ \hat{\boldsymbol{n}} \cdot \hat{\nabla}\hat{\varphi}]_{\hat{\Gamma}} = 0, \tag{2.9b}$$

where $\hat{\nabla}\hat{\varphi} = (\partial_{\hat{x}}\hat{\varphi}, \partial_{\hat{y}}\hat{\varphi})^t$ and $\hat{\boldsymbol{n}} = \mathbf{J}\boldsymbol{n}$ is, in general, not normal to $\hat{\Gamma}$.

Next, we discuss how to translate the extended interface jump conditions (2.5c) and (2.6) to the reference element $\hat{T}$. By the chain rule $\nabla\varphi = \mathbf{J}^t\hat{\nabla}\hat{\varphi}$, we obtain

$$\Delta\varphi = \nabla \cdot \nabla\varphi = (\mathbf{J}^t\hat{\nabla}) \cdot (\mathbf{J}^t\hat{\nabla})\hat{\varphi}. \tag{2.10}$$

Hence, on $\hat{T}$, the extended jump condition (2.5c) becomes

$$[\hat{\beta}(\mathbf{J}^t\hat{\nabla}) \cdot (\mathbf{J}^t\hat{\nabla})\hat{\varphi}]|_{\hat{\Gamma}} = 0. \tag{2.11}$$

We further note that the second normal derivative can be written as

$$\frac{\partial^2 \varphi}{\partial \boldsymbol{n}^2} = (\boldsymbol{n} \cdot \nabla)(\boldsymbol{n} \cdot \nabla)\varphi. \tag{2.12}$$

Thus, (2.6) leads to the following condition on $\hat{T}$:

$$[\hat{\beta}(\hat{\boldsymbol{n}} \cdot \hat{\nabla})(\hat{\boldsymbol{n}} \cdot \hat{\nabla})\hat{\varphi}]|_{\hat{\Gamma}} = [\hat{\beta}\frac{\partial^2 \hat{\varphi}}{\partial \hat{\boldsymbol{n}}^2}]_{\hat{\Gamma}} = 0. \tag{2.13}$$

Therefore, on a reference element $\hat{T}$, we need to construct the following function spaces:

$$\hat{\mathcal{R}}_1^2(\hat{T}) = \{\hat{U} \in \hat{\mathcal{P}}_2(\hat{T}) \mid [\hat{U}]_{\hat{\Gamma}} = 0, [\hat{\beta}\frac{\partial \hat{U}}{\partial \hat{\boldsymbol{n}}}]_{\hat{\Gamma}} = 0, [\hat{\beta}(\mathbf{J}^t\nabla) \cdot (\mathbf{J}^t\nabla)\hat{U}]_{\hat{\Gamma}} = 0\}, \tag{2.14}$$

and

$$\hat{\mathcal{R}}_2^2(\hat{T}) = \{\hat{U} \in \hat{\mathcal{P}}_2(\hat{T}) \mid [\hat{U}]_{\hat{\Gamma}} = 0, [\hat{\beta}\frac{\partial \hat{U}}{\partial \hat{\boldsymbol{n}}}]_{\hat{\Gamma}} = 0, [\hat{\beta}\frac{\partial^2 \hat{U}}{\partial \hat{\boldsymbol{n}}^2}]_{\hat{\Gamma}} = 0\}, \tag{2.15}$$

where

$$\hat{\mathcal{P}}_2 = \{\hat{p} \mid \hat{p}|_{\hat{T}^i} \in \mathcal{P}_2\}. \tag{2.16}$$

2.2. Properties of quadratic IFE spaces. We will now discuss the properties of the IFE spaces $\hat{\mathcal{R}}_k^2(\hat{T}),\ k = 1, 2$, determine their dimensions, and show how to construct their bases. In the discussion below, we note that any piecewise quadratic polynomial on $\hat{T}$ can be written as

$$\hat{p}(\hat{x}, \hat{y}) = \begin{cases} \displaystyle\sum_{i=1}^{6} c_i \hat{L}_i(\hat{x}, \hat{y}), & \text{on } \hat{T}^1, \\ \displaystyle\sum_{i=1}^{6} c_{i+6} \hat{L}_i(\hat{x}, \hat{y}), & \text{on } \hat{T}^2, \end{cases} \tag{2.17}$$

where $\hat{L}_j,\ j = 1, 2, \ldots, 6$, are the standard Lagrange quadratic shape functions on $\hat{T}$ associated with nodes $\hat{V}_i,\ i = 1, 2, \ldots, 6$.

Let T be an arbitrary interface triangle and let $\hat{T} = F(T)$ be the associated reference triangle cut by the interface $\hat{\Gamma} : \hat{y} = a\hat{x} + b$, as illustrated in Figure 2.2. We recall that F is the standard affine mapping given in (2.7) and that the unit normal vector $\boldsymbol{n}$ to the physical interface Γ is mapped to $\hat{\boldsymbol{n}} = \mathbf{J}\boldsymbol{n}$ which, in general, is not normal to $\hat{\Gamma}$.

In the next lemma we show that $\hat{\boldsymbol{n}} = (\hat{n}_x, \hat{n}_y)^t$ cannot be parallel to $\hat{\Gamma}$ when F is an invertible affine mapping.

Lemma 2.1. *Let T be an arbitrary interface element cut by a linear interface Γ. If F is the standard affine mapping from T to the reference element $\hat{T}$, then*

$$a\hat{n}_x - \hat{n}_y \neq 0. \tag{2.18}$$

Proof. First, the unit normal vector to the interface $\hat{\Gamma}$ defined by the equation $\hat{y} = a\hat{x} + b$ can be written as

$$\hat{\mathbf{N}} = \frac{1}{\sqrt{1 + a^2}}(a, -1)^t$$

with inner product

$$\hat{\boldsymbol{n}} \cdot \hat{\mathbf{N}} = \frac{a\hat{n}_x - \hat{n}_y}{\sqrt{1 + a^2}}. \tag{2.19}$$

Assume $\hat{\boldsymbol{n}}$ to be parallel to $\hat{\Gamma}$, then the inner product $\hat{\boldsymbol{n}} \cdot \hat{\mathbf{N}} = 0$. Hence the line containing Γ and all lines perpendicular to it are mapped onto the line containing $\hat{\Gamma}$. This means F maps $\mathbb{R}^2$ onto the line containing $\hat{\Gamma}$. This contradicts the one-to-one property of F and proves the lemma. □

Properties of $\hat{\mathcal{R}}_k^2(\hat{T}), k = 1, 2$: First, we prove that $\hat{\mathcal{R}}_k^2(\hat{T}), k = 1, 2$ is a nontrivial space with dimension 6.

Lemma 2.2. *Let $\hat{p} \in \hat{\mathcal{P}}_2$ be defined by (2.17) with coefficients $\mathbf{c} = (c_1, c_2, \ldots, c_{12})^t \in \mathbb{R}^{12}$ and $P_1 = \hat{E}$, $P_2 = \hat{D}$ and $P_3 = (\hat{D} + \hat{E})/2$ as illustrated in Figure 2.2. Then*

$$\hat{p} \in \hat{\mathcal{R}}_k^2(\hat{T}) \quad \text{if and only if} \quad \mathbf{c} \in N(\mathbf{A}(k)),\ k = 1, 2, \tag{2.20}$$

where $N(\mathbf{A}(k))$ is the null space of the 6×12 rectangular matrix $\mathbf{A}(k)$ defined by

$$\mathbf{A}(k) = \begin{pmatrix} \mathbf{A}_0 & -\mathbf{A}_0 \\ \mathbf{A}_1 & -r\mathbf{A}_1 \\ \mathbf{A}_{2,k} & -r\mathbf{A}_{2,k} \end{pmatrix},\ k = 1, 2 \tag{2.21a}$$

with $r = \frac{\hat{\beta}^2}{\hat{\beta}^1}$ and

$$\mathbf{A}_0 = \begin{pmatrix} \hat{L}_1(P_1) & \hat{L}_2(P_1) & \hat{L}_3(P_1) & \hat{L}_4(P_1) & \hat{L}_5(P_1) & \hat{L}_6(P_1) \\ \hat{L}_1(P_2) & \hat{L}_2(P_2) & \hat{L}_3(P_2) & \hat{L}_4(P_2) & \hat{L}_5(P_2) & \hat{L}_6(P_2) \\ \hat{L}_1(P_3) & \hat{L}_2(P_3) & \hat{L}_3(P_3) & \hat{L}_4(P_3) & \hat{L}_5(P_3) & \hat{L}_6(P_3) \end{pmatrix}, \tag{2.21b}$$

$$\mathbf{A}_1 = \begin{pmatrix} \frac{\partial \hat{L}_1}{\partial \hat{\boldsymbol{n}}}(P_1) & \frac{\partial \hat{L}_2}{\partial \hat{\boldsymbol{n}}}(P_1) & \frac{\partial \hat{L}_3}{\partial \hat{\boldsymbol{n}}}(P_1) & \frac{\partial \hat{L}_4}{\partial \hat{\boldsymbol{n}}}(P_1) & \frac{\partial \hat{L}_5}{\partial \hat{\boldsymbol{n}}}(P_1) & \frac{\partial \hat{L}_6}{\partial \hat{\boldsymbol{n}}}(P_1) \\ \frac{\partial \hat{L}_1}{\partial \hat{\boldsymbol{n}}}(P_2) & \frac{\partial \hat{L}_2}{\partial \hat{\boldsymbol{n}}}(P_2) & \frac{\partial \hat{L}_3}{\partial \hat{\boldsymbol{n}}}(P_2) & \frac{\partial \hat{L}_4}{\partial \hat{\boldsymbol{n}}}(P_2) & \frac{\partial \hat{L}_5}{\partial \hat{\boldsymbol{n}}}(P_2) & \frac{\partial \hat{L}_6}{\partial \hat{\boldsymbol{n}}}(P_2) \end{pmatrix}, \tag{2.21c}$$

$$\mathbf{A}_{2,1} = \begin{pmatrix} a_1 & a_2 & \ldots & a_6 \end{pmatrix},\ a_j = (\mathbf{J}^t \nabla) \cdot (\mathbf{J}^t \nabla) \hat{L}_j(P_1),\ 1 \le j \le 6. \tag{2.21d}$$

$$\mathbf{A}_{2,2} = \begin{pmatrix} \frac{\partial^2 \hat{L}_1}{\partial \hat{\boldsymbol{n}}^2}(P_1) & \frac{\partial^2 \hat{L}_2}{\partial \hat{\boldsymbol{n}}^2}(P_1) & \frac{\partial^2 \hat{L}_3}{\partial \hat{\boldsymbol{n}}^2}(P_1) & \frac{\partial^2 \hat{L}_4}{\partial \hat{\boldsymbol{n}}^2}(P_1) & \frac{\partial^2 \hat{L}_5}{\partial \hat{\boldsymbol{n}}^2}(P_1) & \frac{\partial^2 \hat{L}_6}{\partial \hat{\boldsymbol{n}}^2}(P_1) \end{pmatrix}. \tag{2.21e}$$

Proof. We present a proof for the case $k = 2$. Similar arguments can be used for $k = 1$ and we refer readers to [7] for related details.

We first show that the condition is necessary. Assume that $\hat{p} \in \hat{\mathcal{R}}_2^2(\hat{T})$, then

$$[\hat{p}]_{\hat{\Gamma}} = 0,\ [\hat{\beta} \frac{\partial \hat{p}}{\partial \hat{\boldsymbol{n}}}]_{\hat{\Gamma}} = 0,\ [\hat{\beta} \frac{\partial^2 \hat{p}}{\partial \hat{\boldsymbol{n}}^2}]_{\hat{\Gamma}} = 0. \tag{2.22}$$

The jump condition specified by the first equation in (2.22) is equivalent to enforcing $[\hat{p}](P_i) = 0,\ i = 1, 2, 3$, which can be written as

$$\sum_{j=1}^{6} c_j \hat{L}_j(P_i) - \sum_{j=1}^{6} c_{j+6} \hat{L}_j(P_i) = 0,\ i = 1, 2, 3,$$

or

$$\left(\mathbf{A}_0, -\mathbf{A}_0\right) \mathbf{c} = 0. \tag{2.23}$$

Similarly, the jump condition described by the second equation in (2.22) is equivalent to $[\hat{\beta}\frac{\partial \hat{p}}{\partial \hat{\boldsymbol{n}}}](P_i) = 0,\ i = 1, 2$, which can be written as

$$\sum_{j=1}^{6} c_j \frac{\partial \hat{L}_j}{\partial \hat{\boldsymbol{n}}}(P_i) - r \sum_{j=1}^{6} c_{j+6} \frac{\partial \hat{L}_j}{\partial \hat{\boldsymbol{n}}}(P_i) = 0,\ i = 1, 2,$$

or

$$\left(\mathbf{A}_1, -r\mathbf{A}_1\right) \mathbf{c} = 0. \tag{2.24}$$

The third equation in (2.22) is equivalent to $[\hat{\beta}\frac{\partial^2 \hat{p}}{\partial \hat{\boldsymbol{n}}^2}](P_1) = 0$, which can be written as

$$\sum_{j=1}^{6} c_j \frac{\partial^2 \hat{L}_j}{\partial \hat{\boldsymbol{n}}^2}(P_1) - r \sum_{j=1}^{6} c_{j+6} \frac{\partial^2 \hat{L}_j}{\partial \hat{\boldsymbol{n}}^2}(P_1) = 0.$$

This is equivalent

$$\left(\mathbf{A}_{2,2}, -r\mathbf{A}_{2,2}\right) \mathbf{c} = 0. \tag{2.25}$$

Combining (2.23), (2.24) and (2.25) yields $\mathbf{A}(2)\mathbf{c} = 0$.

Reversing the arguments above can show that the condition is also sufficient. □

In the next lemma we show that the nullity of $\mathbf{A}(k), k = 1, 2$ defined in (2.21) is equal to 6.

Lemma 2.3. *Under the assumptions of Lemma 2.2, the nullity of the matrix* $\mathbf{A}(k), k = 1, 2$ *defined in (2.21) is equal to 6.*

Proof. We present a proof for the case $k = 2$, and we refer readers to [7] for related arguments when $k = 1$. Let us consider the 6×6 submatrix of $\mathbf{A}(2)$

$$\mathbf{A}_c = \begin{pmatrix} \mathbf{A}_0 \\ \mathbf{A}_1 \\ \mathbf{A}_{2,2} \end{pmatrix}. \tag{2.26}$$

A direct calculation gives its determinant as follows:

$$det(\mathbf{A}_c) = \frac{32}{(1+a)^4}(1-b)^4(a\hat{n}_x - \hat{n}_y)^4. \tag{2.27}$$

By the fact $b \neq 1$ and Lemma 2.1 we can show that $\mathbf{A}_c$ is invertible, hence, the rank of $\mathbf{A}(2)$ is equal to 6. Then, we finish the proof by applying the rank-nullity theorem:

$$rank(\mathbf{A}(2)) + nullity(\mathbf{A}(2)) = 12. \tag{2.28}$$

□

In the next lemma we establish the existence of an isomorphism between $\hat{\mathcal{R}}_k^2(\hat{T})$ and $N(\mathbf{A}(k))$ for $k = 1, 2$.

Theorem 2.1. *Let* $\mathbf{A}(k), k = 1, 2$ *be the matrix defined by (2.21). Then the following statements hold for* $k = 1, 2$.

1. *There exists an isomorphism* Ψ *from the quadratic IFE space* $\hat{\mathcal{R}}_k^2(\hat{T})$ *to the null space* $N(\mathbf{A}(k))$.
2. *The dimension of* $\hat{\mathcal{R}}_k^2(\hat{T})$ *is equal to 6.*
3. *A set of vectors* $\{\mathbf{b}_i,\ i = 1, 2, \ldots, 6\} \subset \mathbb{R}^{12}$ *form a basis of* $N(\mathbf{A}(k))$ *if and only if* $\{\Psi^{-1}(\mathbf{b}_i),\ i = 1, 2, \ldots, 6\}$ *form a basis of* $\hat{\mathcal{R}}_k^2(\hat{T})$.

Proof. Again, we present a proof for the case $k = 2$, and we refer readers to [7] for related arguments when $k = 1$.

Since each $\hat{p} \in \hat{\mathcal{R}}_2^2(\hat{T})$ can be represented in the form given in (2.17), we define the mapping $\Psi : \hat{\mathcal{R}}_2^2(\hat{T}) \to N(\mathbf{A}(2))$ by

$$\Psi(\hat{p}) = (c_1, c_2, \ldots, c_{12})^t. \tag{2.29}$$

From the definition of Ψ, one can easily show that Ψ is linear, *i.e.*,

$$\Psi(\lambda \boldsymbol{a} + \mu \mathbf{b}) = \lambda \Psi(\boldsymbol{a}) + \mu \Psi(\mathbf{b}),\ \forall\ \boldsymbol{a}, \mathbf{b} \in \mathbb{R}^{12} \text{ and } \lambda, \mu \in \mathbb{R}. \tag{2.30}$$

Establishing that Ψ is injective is straightforward by setting $\Psi(\hat{p}) = \Psi(\hat{q})$ we show that $\hat{p} = \hat{q}$.

Next, we show that Ψ is surjective. In fact, for every $\mathbf{c} = (c_1, c_2, \ldots, c_{12})^t \in N(\mathbf{A}(2))$, by Lemma 2.2, we can define a piecewise quadratic polynomial $\hat{p} \in \hat{\mathcal{R}}_2^2(\hat{T})$ of the form (2.17). Thus, for all $\mathbf{c} \in N(\mathbf{A}(2))$ there exists $\hat{p} \in \hat{\mathcal{R}}_2^2(\hat{T})$ such that $\Psi(\hat{p}) = \mathbf{b}$.

Hence, the mapping Ψ is an isomorphism between $\hat{\mathcal{R}}_2^2(\hat{T})$ and $N(\mathbf{A}(2))$. Using Lemma 2.3 yields $dim(\hat{\mathcal{R}}_2^2(\hat{T})) = dim(N(\mathbf{A}(2))) = 6$.

Since Ψ is an isomorphism, each basis of $N(\mathbf{A}(2))$ is mapped into a basis of $\hat{\mathcal{R}}_2^2(\hat{T})$ which completes the proof. □

In conclusion, both quadratic IFE spaces $\hat{\mathcal{R}}_k^2(\hat{T}),\ k = 1, 2$, have dimension six and their elements can be represented as linear combinations of the piecewise quadratic basis functions obtained from a basis of the corresponding null space $N(\mathbf{A}(k))$.

More conventional basis functions such as Lagrange and hierarchical shape functions may be constructed for these interface spaces. The existence and uniqueness of such shape functions will be discussed in the next section.

2.3. Quadratic IFE shape functions. Now we will construct Lagrange and hierarchical shape functions for IFE spaces introduced above.

2.3.1. IFE shape functions of Lagrange type. Let $\hat{T}$ be a reference interface element of any of the three types described in Figure 2.2. In this section, we consider a basis for $\hat{\mathcal{R}}_k^2(\hat{T}),\ k = 1, 2$, consisting of the IFE shape functions of Lagrange type $\hat{\varphi}_i \in \hat{\mathcal{R}}_k^2(\hat{T}),\ i = 1, 2, \ldots, 6,\ k = 1, 2$, satisfying the nodal constraints

$$\hat{\varphi}_i(\hat{V}_j) = \delta_{ij},\ j = 1, 2, \ldots, 6. \tag{2.31}$$

First, we construct a line perpendicular to line Γ and we denote it by $\Gamma^{\perp}$. Then we use these two lines to form an interface coordinate for representing each point (x, y) as follows:

$$\begin{cases} \xi = \xi(x, y) = & \frac{1}{\sqrt{1+A^2}}\ (x + Ay + C), \\ \eta = \eta(x, y) = & \frac{1}{\sqrt{1+A^2}}\ (y - Ax - B), \end{cases} \tag{2.32}$$

where η is the distance between (x, y) and Γ and C is a constant chosen such that $(\xi(0, B), \eta(0, B)) = (0, 0)$. Through the mapping $F : T \to \hat{T}$, the interface Γ becomes $\hat{\Gamma} = F(\Gamma)$ defined by $\hat{y} = a\hat{x} + b$, and $\Gamma^{\perp}$ becomes $\widehat{\Gamma^{\perp}} = F(\Gamma^{\perp})$ which is parallel to the line given by $\hat{n}_{\hat{x}}\hat{y} - \hat{n}_{\hat{y}}\hat{x} + c = 0$, where $(\hat{n}_{\hat{x}}, \hat{n}_{\hat{y}})^t = \hat{\boldsymbol{n}} = \mathbf{J}\boldsymbol{n}$. These two lines in the $\hat{x}$-$\hat{y}$ plane form, in general, a skew coordinate system as illustrated in Figure 2.3. We can use it to represent a point $(\hat{x}, \hat{y})$ as follows:

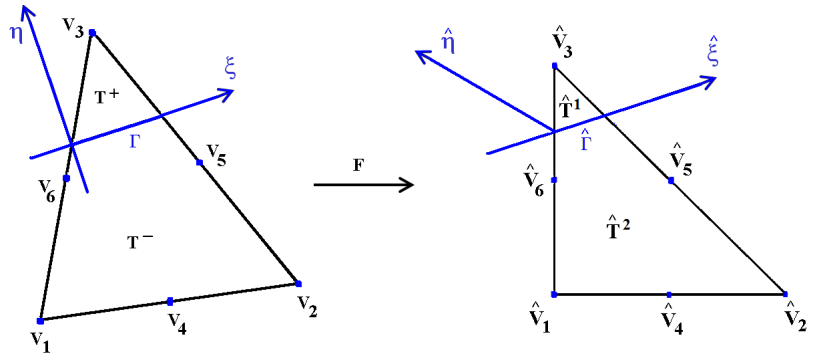

FIGURE 2.3. The interface coordinates systems (ξ, η) on T and $(\hat{\xi}, \hat{\eta})$ on $\hat{T} = F(T)$.

$$\begin{cases} \hat{\xi} = & \hat{\xi}(\hat{x}, \hat{y}), \\ \hat{\eta} = & \hat{\eta}(\hat{x}, \hat{y}) \end{cases} \tag{2.33}$$

where both $\hat{\xi}(\hat{x}, \hat{y})$ and $\hat{\eta}(\hat{x}, \hat{y})$ are linear functions of $\hat{x}$ and $\hat{y}$, and $\hat{\Gamma}$ is described by $\hat{\eta} = 0$.

We now describe how to use the interface coordinates $(\hat{\xi}, \hat{\eta})$ on the reference element to construct a shape function in $\hat{\mathcal{R}}_2^2(\hat{T})$. First, we define the following sets of indices: $\mathscr{I}_1$ the set of indices of all nodes of $\hat{T}$ in $\hat{T}^1$, and $\mathscr{I}_2$ the set of indices of all nodes of $\hat{T}$ in $\hat{T}^2$. Hence, considering the 3 types of reference elements shown in the first row of Figure 2.2, if $\hat{T}$ is of type I, $\mathscr{I}_1 = \{3\}$ and $\mathscr{I}_2 = \{1, 2, 4, 5, 6\}$; if $\hat{T}$ is of type II, $\mathscr{I}_1 = \{3, 5\}$ and $\mathscr{I}_2 = \{1, 2, 4, 6\}$; and if $\hat{T}$ is of type III, $\mathscr{I}_1 = \{3, 5, 6\}$ and $\mathscr{I}_2 = \{1, 2, 4\}$.

Then, following the idea proposed by Adjerid and Lin [3] for one-dimensional lagrange IFE shape functions, we now discuss how to construct the shape functions $\hat{\varphi}_i,\ i = 1, 2, \ldots, 6$ in terms of the standard quadratic shape functions of Lagrange type $\hat{L}_j(\hat{x}, \hat{y}),\ j = 1, 2, \ldots, 6$ on the reference element. First, given a function $\bar{\phi}(\hat{\xi}, \hat{\eta})$ we can consider a function of $(\hat{x}, \hat{y})$: $\hat{\phi}(\hat{x}, \hat{y}) = \bar{\phi}(\hat{\xi}(\hat{x}, \hat{y}), \hat{\eta}(\hat{x}, \hat{y}))$ where one can verify that

$$\frac{\partial \hat{\phi}(\hat{x}, \hat{y})}{\partial \hat{\boldsymbol{n}}} = C \frac{\partial \bar{\phi}(\hat{\xi}(\hat{x}, \hat{y}), \hat{\eta}(\hat{x}, \hat{y}))}{\partial \hat{\eta}} \tag{2.34}$$

with C being a generic constant. This property can be used to construct a piecewise quadratic function to satisfy the interface jump conditions. For instance, given the expression $\bar{\varphi}^{(1)}(\hat{\xi}, \hat{\eta})$ on $\hat{T}^1$, we can extend it to a function $\bar{\varphi}$ on the whole $\hat{T}$ by defining its expression on $\hat{T}^2$ as

$$\bar{\varphi}^{(2)}(\hat{\xi}, \hat{\eta}) = \bar{\varphi}^{(1)}(\hat{\xi}, 0) + \frac{\hat{\beta}^1}{\hat{\beta}^2} \left(\bar{\varphi}^{(1)}(\hat{\xi}, \hat{\eta}) - \bar{\varphi}^{(1)}(\hat{\xi}, 0) \right). \tag{2.35}$$

Let $\hat{\pi}(\hat{x}, \hat{y})$ be the image of $(\hat{x}, \hat{y})$ by the oblique projection parallel to the $\hat{\eta}$ axis on $\hat{\Gamma}$ and let $\hat{\varphi}(\hat{x}, \hat{y}) = \bar{\varphi}(\hat{\xi}, \hat{\eta})$. Then,

$$\hat{\varphi}^{(2)}(\hat{x}, \hat{y}) = \frac{\hat{\beta}^1}{\hat{\beta}^2} \hat{\varphi}^{(1)}(\hat{x}, \hat{y}) + \left(1 - \frac{\hat{\beta}^1}{\hat{\beta}^2} \right) \tilde{\varphi}_i^1(\hat{x}, \hat{y}), \tag{2.36}$$

with $\tilde{\varphi}_i^{(1)}(\hat{x},\hat{y}) = \bar{\varphi}_i^{(1)}(\hat{\pi}(\hat{x},\hat{y}))$. By (2.34), we can show that $\hat{\varphi}(\hat{x},\hat{y})$ satisfies the jump conditions required by $\hat{\mathcal{R}}_2^2(\hat{T})$.

Hence, for each of the shape functions $\hat{\varphi}_i,\ i = 1,2,\ldots,6$, we first determine one of its two expressions such that it has zero values at all nodes on one side of $\hat{T}$. Then, we use this extension technique to determine the formula of this shape function on the other side of $\hat{T}$ such that pertinent interface jump conditions and nodal value constraints are satisfied. Specifically, let $\hat{r} = \frac{\hat{\beta}^1}{\hat{\beta}^2}$, then we can form $\hat{\varphi}_i \in \hat{\mathcal{R}}_2^2(\hat{T}),\ i = 1,2,\ldots,6$ as follows.

For $i \in \mathscr{I}_1$ we write the shape function $\hat{\varphi}_i$ as

$$\hat{\varphi}_i(\hat{x},\hat{y}) = \begin{cases} \hat{\varphi}_i^{(2)}(\hat{x},\hat{y}) = \sum\limits_{j\in\mathscr{I}_1} c_j \hat{L}_j(\hat{x},\hat{y}) , & (\hat{x},\hat{y}) \in \hat{T}^2, \\ \hat{\varphi}_i^{(1)}(\hat{x},\hat{y}) = \frac{1}{\hat{r}}\ \hat{\varphi}_i^{(2)}(\hat{x},\hat{y}) + (1-\frac{1}{\hat{r}})\ \tilde{\varphi}_i^{(2)}(\hat{x},\hat{y}) , & (\hat{x},\hat{y}) \in \hat{T}^1, \end{cases} \tag{2.37}$$

and for $i \in \mathscr{I}_2$, we write the shape function $\hat{\varphi}_i$ as

$$\hat{\varphi}_i(\hat{x},\hat{y}) = \begin{cases} \hat{\varphi}_i^{(1)}(\hat{x},\hat{y}) = \sum\limits_{j\in\mathscr{I}_2} c_j \hat{L}_j(\hat{x},\hat{y}) , & (\hat{x},\hat{y}) \in \hat{T}^1, \\ \hat{\varphi}_i^{(2)}(\hat{x},\hat{y}) = \hat{r}\ \hat{\varphi}_i^{(1)}(\hat{x},\hat{y}) + (1-\hat{r})\ \tilde{\varphi}_i^{(1)}(\hat{x},\hat{y}) , & (\hat{x},\hat{y}) \in \hat{T}^2. \end{cases} \tag{2.38}$$

Here $\tilde{\varphi}_i^{(k)} = \hat{\varphi}_i^{(k)} \circ \hat{\pi},\ k = 1,2$ and the coefficients $c_j, j \in \mathscr{I}_k, k = 1,2$ are further determined by imposing the Lagrange nodal value conditions (2.31). Later in this section, we will show that these coefficients and their corresponding shape function $\hat{\varphi}_i,\ i = 1,2,\ldots,6$ can be uniquely determined.

Similar ideas can be applied to construct shape functions $\hat{\varphi}_i,\ i = 1,2,\ldots,6$ for the IFE space $\hat{\mathcal{R}}_1^2(\hat{T})$ as follows.

For $i \in \mathscr{I}_1$, we write the shape function $\hat{\varphi}_i$ as

$$\hat{\varphi}_i(\hat{x},\hat{y}) = \begin{cases} \hat{\varphi}_i^{(2)}(\hat{x},\hat{y}) = \sum\limits_{j\in\mathscr{I}_1} c_j \hat{L}_j(\hat{x},\hat{y}), & (\hat{x},\hat{y}) \in \hat{T}^2, \\ \hat{\varphi}_i^{(1)}(\hat{x},\hat{y}) = \frac{1}{\hat{r}}\ \hat{\varphi}_i^{(2)}(\hat{x},\hat{y}) + (1-\frac{1}{\hat{r}})\tilde{\varphi}_i^{(2)}(\hat{x},\hat{y}) \\ \qquad\qquad - (1-\frac{1}{\hat{r}})\ \frac{(\hat{y}-a\hat{x}-b)^2}{2(1+a^2)}\hat{\Delta}\tilde{\varphi}_i^{(2)}(\hat{x},\hat{y}), & (\hat{x},\hat{y}) \in \hat{T}^1, \end{cases}$$

and for $i \in \mathscr{I}_2$, we write the shape function $\hat{\varphi}_i$ as

$$\hat{\varphi}_i(\hat{x},\hat{y}) = \begin{cases} \hat{\varphi}_i^{(1)}(\hat{x},\hat{y}) = \sum\limits_{j\in\mathscr{I}_2} c_j \hat{L}_j(\hat{x},\hat{y}), & (\hat{x},\hat{y}) \in \hat{T}^1, \\ \hat{\varphi}_i^{(2)}(\hat{x},\hat{y}) = \hat{r}\ \hat{\varphi}_i^{(1)}(\hat{x},\hat{y}) + (1-\hat{r})\tilde{\varphi}_i^{(1)}(\hat{x},\hat{y}) \\ \qquad\qquad - (1-\hat{r})\ \frac{(\hat{y}-a\hat{x}-b)^2}{2(1+a^2)}\hat{\Delta}\tilde{\varphi}_i^{(1)}(\hat{x},\hat{y}), & (\hat{x},\hat{y}) \in \hat{T}^2, \end{cases}$$

with $\hat{\Delta} = (\mathbf{J}^t\hat{\nabla})\cdot(\mathbf{J}^t\hat{\nabla})$.

The following theorem is about the existence and uniqueness of the shape functions for $\hat{\mathcal{R}}_2^2(\hat{T})$. Similar result can be established for IFE space $\mathcal{R}_1^2(T)$ with a little more computations.

Theorem 2.2. *Let $\hat{T}$ be a reference interface element cut by the interface $\hat{\Gamma} : \hat{y} = a\hat{x} + b$, and let $\hat{\mathcal{R}}_2^2(\hat{T})$ be the piecewise quadratic polynomial space defined in (2.15) with $\hat{\boldsymbol{n}}$ orthogonal to $\hat{\Gamma}$. Then, there exist six shape functions $\hat{\varphi}_i$, $i = 1,2,\ldots,6$, in*

$\hat{\mathcal{R}}_2^2(\hat{T})$ *satisfying the Lagrange nodal value conditions (2.31). The shape functions* $\hat{\varphi}_i,\ i = 1, 2, \ldots, 6$, *are unique.*

Proof. The proof is elementary which is basically to show that nodal value constraints imposed on each $\hat{\varphi}_i,\ i = 1, 2, \ldots, 6$ lead to a linear system about coefficients in (2.37) or (2.38) and the matrix in this linear system is nonsingular. Readers can refer [7] for more details.

□

Corollary 2.1. *Under the assumptions of Theorem 2.2, the shape functions* $\hat{\varphi}_i \in \hat{\mathcal{R}}_2^2(\hat{T}),\ i = 1, 2, \ldots, 6$, *satisfying the Lagrange nodal value conditions* $\hat{\varphi}_i(\hat{V}_j) = \delta_{ij},\ i, j = 1, 2, \ldots, 6$, *form a basis of* $\hat{\mathcal{R}}_2^2(\hat{T})$.

Proof. The conditions $\hat{\varphi}_i(\hat{V}_j) = \delta_{ij},\ i, j = 1, 2, \ldots, 6$, trivially imply the linear independence of $\hat{\varphi}_i,\ i = 1, 2, \ldots, 6$. Since the dimension of $\hat{\mathcal{R}}_2^2(\hat{T})$ is equal to 6, then the result follows. □

Corollary 2.2. *Under the assumptions of Theorem 2.2,* $\hat{\varphi}_i,\ i = 1, 2, \ldots, 6$ *form a partition of unity for the space* $\hat{\mathcal{R}}_2^2(\hat{T})$, *i.e.*

$$\sum_{i=1}^{6} \hat{\varphi}_i(\hat{x}, \hat{y}) = 1, \qquad \forall (\hat{x}, \hat{y}) \in \hat{T}. \tag{2.39}$$

Proof. Let $\hat{\varphi}_i,\ i = 1, 2, \ldots, 6$ be the Lagrange basis of $\hat{\mathcal{R}}_2^2(\hat{T})$. Since the constant function $\hat{\varphi}_0(\hat{x}, \hat{y}) = 1$ is in $\hat{\mathcal{R}}_2^2(\hat{T})$, then, there exists $d_i,\ i = 1, 2, \ldots, 6$ such that

$$\sum_{i=1}^{6} d_i \hat{\varphi}_i(\hat{x}, \hat{y}) = \hat{\varphi}_0(\hat{x}, \hat{y}) = 1. \tag{2.40}$$

Since $\hat{\varphi}_i(\hat{V}_j) = \delta_{ij},\ i, j = 1, 2, \ldots, 6$, evaluating equation (2.40) at $\hat{V}_j$ implies $d_j = 1,\ j = 1, 2, \ldots, 6$, which completes the proof. □

Next, we make few observations:

(1) The previous existence and uniqueness proofs extend to any isosceles right triangle interface element T in a straightforward manner by noting that such triangle may be mapped into one of the reference triangles by a composition of a translation, a rotation, a dilation, and a reflection which preserve the right angle. Thus, the image $\hat{\boldsymbol{n}}$ of the normal vector $\boldsymbol{n}$ is orthogonal to the image $\hat{\Gamma}$ of the interface Γ.

(2) From Theorem 2.2, we conclude the existence of six shape functions $\hat{\varphi}_i,\ i = 1, 2, \ldots, 6$ in $\hat{\mathcal{R}}_2^2(\hat{T})$ that are uniquely determined by the Lagrange nodal value conditions. Since $dim(\mathcal{R}_2^2(T)) = 6$, and the shape functions
$$\varphi_i(x, y) = \hat{\varphi}_i(F(x, y)) \in \mathcal{R}_2^2(T), \quad i = 1, 2, \ldots, 6,$$
are linearly independent, thus, they form a basis of $\mathcal{R}_2^2(T)$.

(3) The assumption of uniform meshes with isosceles right triangular elements is an acceptable assumption, since the IFE method may, in general, be used on uniform Cartesian meshes independent of the interface.

Next, we define the global Lagrange type quadratic IFE spaces over the whole domain Ω. Locally, on every non-interface element T, we let $\mathcal{R}_k^2(T) = \mathcal{P}_2, k = 1, 2$, spanned by standard Lagrange shape functions. Let $\mathcal{N}_h$ be the set of nodes for the standard Lagrange quadratic finite element space defined on the triangular mesh

$\mathcal{T}_h$. At each node $\mathbf{v}_i \in \mathcal{N}_h$, we define a piecewise quadratic IFE basis functions $\psi_i^{(k)}$ for $k = 1, 2$, respectively, over the whole domain such that for $k = 1, 2$,

$$\psi_i^{(k)}|_T \in \mathcal{R}_k^2(T), \text{ for } T \in \mathcal{T}_h, \text{ and } \psi_i^{(k)}(\mathbf{v}_j) = \delta_{ij}, \ \forall\ \mathbf{v}_j \in \mathcal{N}_h.$$

The global quadratic IFE basis functions constructed above may be discontinuous across interface edges as illustrated in Figure 2.4. More precisely, the global IFE basis functions are continuous across non-interface edges while, in general, they are continuous only at the two edge vertices and midpoint of an interface edge.

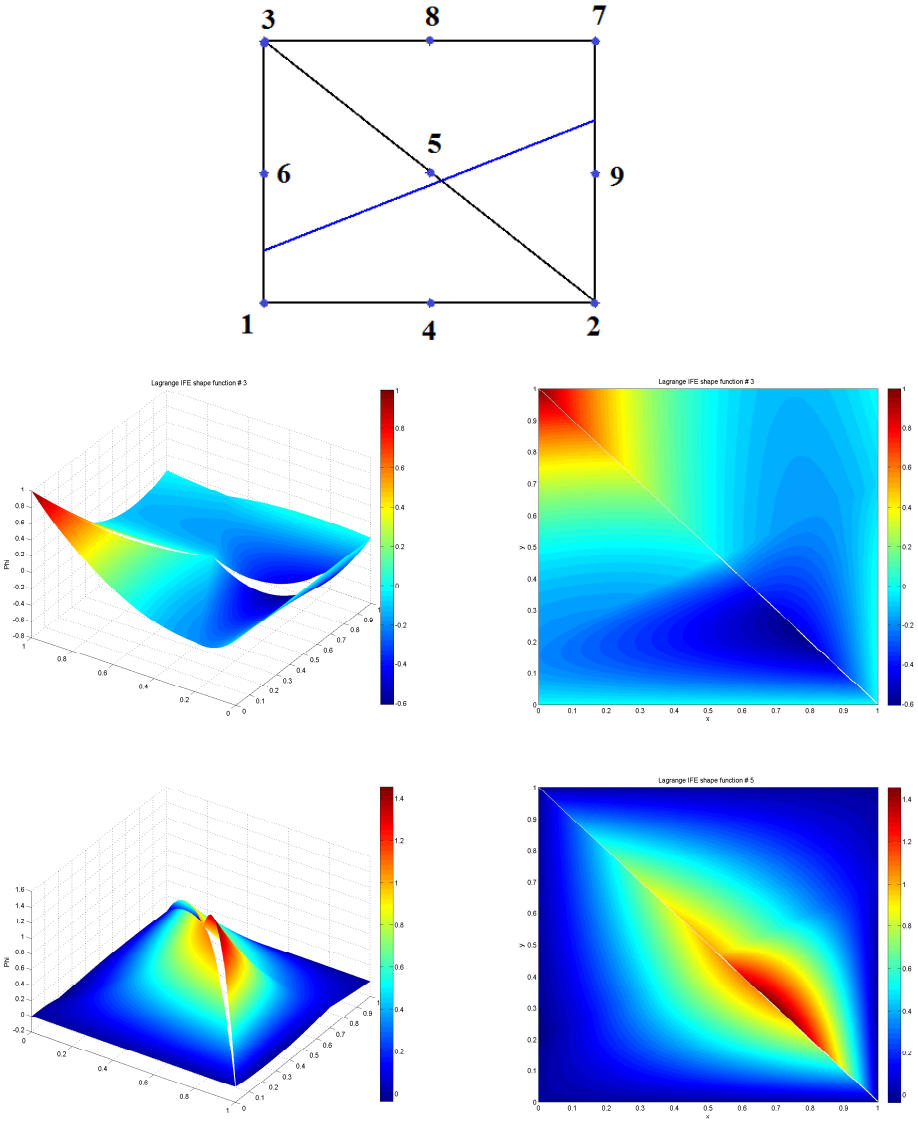

FIGURE 2.4. A mesh having two elements for $\Omega = (0, 1)^2$ cut by the interface $y = x/2 + 1/5$ with $r = 5$ (top) and Lagrange immersed basis functions $\psi_3^{(2)}$(middle) and $\psi_5^{(2)}$(bottom).

Without loss of generality, we assume that $\mathcal{N}_h$ contains N nodes among which the first N_I nodes are in the interior of Ω while the rest of them are on the boundary of Ω. Then, finally, we can define the quadratic IFE spaces over the whole domain as

$$\mathcal{S}_h^{2,k} = span\{\psi_j^{(k)},\ j = 1, 2, \ldots, N\},\ k = 1, 2, \tag{2.41}$$

and define the space $\mathcal{S}_{h,0}^{2,k}, k = 1, 2$ to be the IFE spaces associated with interior nodes as follows:

$$\mathcal{S}_{h,0}^{2,k} = span\{\psi_j^{(k)},\ j = 1, 2, \ldots, N_I\},\ k = 1, 2. \tag{2.42}$$

2.3.2. Hierarchical shape functions in $\hat{\mathcal{R}}_k^2(\hat{T}), k = 1, 2$. Hierarchical shape functions have several advantages over their Lagrange counterparts as they yield well conditioned algebraic problems and efficient p-refinement algorithms. In this section we discuss the construction of hierarchical quadratic IFE shape functions by following the standard procedure for classical hierarchical shape functions.

On an interface reference element $\hat{T} = \triangle\hat{V}_1\hat{V}_2\hat{V}_3$, we assume, without loss of generality, that the interface cut through edges $\hat{V}_1\hat{V}_3$ and $\hat{V}_2\hat{V}_3$ as illustrated in Figure 2.3. On this element, there are three piecewise linear Lagrange type IFE shape functions $\hat{\varphi}_i^{(1)},\ i = 1, 2, 3$, that can be described as follows:

$$\hat{\phi}_1^{(1)} = \begin{cases} \hat{\phi}_1^{(1),1} = c_1\hat{L}_1(\hat{x}, \hat{y}) + c_2\hat{L}_2(\hat{x}, \hat{y}), & \text{on } \hat{T}^1, \\ \hat{\phi}_1^{(1),2} = \hat{L}_1(\hat{x}, \hat{y}) + c_3\hat{L}_3(\hat{x}, \hat{y}), & \text{on } \hat{T}^2, \end{cases} \tag{2.43}$$

$$\hat{\phi}_2^{(1)} = \begin{cases} \hat{\phi}_2^{(1),1} = c_1\hat{L}_1(\hat{x}, \hat{y}) + c_2\hat{L}_2(\hat{x}, \hat{y}), & \text{on } \hat{T}^1, \\ \hat{\phi}_2^{(1),2} = \hat{L}_2(\hat{x}, \hat{y}) + c_3\hat{L}_3(\hat{x}, \hat{y}), & \text{on } \hat{T}^2, \end{cases} \tag{2.44}$$

and

$$\hat{\phi}_3^{(1)} = \begin{cases} \hat{\phi}_3^{(1),1} = \hat{L}_3(\hat{x}, \hat{y}) + c_1\hat{L}_1(\hat{x}, \hat{y}) + c_2\hat{L}_2(\hat{x}, \hat{y}), & \text{on } \hat{T}^1, \\ \hat{\phi}_3^{(1),2} = c_3\hat{L}_3(\hat{x}, \hat{y}), & \text{on } \hat{T}^2, \end{cases} \tag{2.45}$$

where, $\hat{L}_i(\hat{x}, \hat{y}), i = 1, 2, 3$ are the standard linear Lagrange shape function on $\hat{T}$, and according to [21], the coefficients $c_1,\ c_2,\ c_3$ for each shape function are uniquely determined by the interface jump conditions (2.9).

Next, we construct three IFE shape functions associated the edges of T for the space $\hat{\mathcal{R}}_1^2(\hat{T})$ as follows. For each 3-tuple $(k, i, j) = (4, 1, 2),\ (5, 2, 3)\ (6, 3, 1)$ we define the IFE shape functions associated with the edge containing the nodes $\hat{V}_k, k = 4, 5, 6$ by

$$\hat{\varphi}_k^{(2)} = \begin{cases} \hat{\varphi}_k^{(2),1} = \hat{\varphi}_i^{(1),1}(\hat{x}, \hat{y})\hat{\varphi}_j^{(1),1}(\hat{x}, \hat{y}) + \ \hat{c}_k\ \frac{(\hat{y} - a\hat{x} - b)^2}{(1+a^2)}\ ,\ (\hat{x}, \hat{y}) \in \hat{T}^1, \\ \hat{\varphi}_k^{(2),2} = \hat{\varphi}_i^{(1),2}(\hat{x}, \hat{y})\hat{\varphi}_j^{(1),2}(\hat{x}, \hat{y})\ , \qquad\qquad (\hat{x}, \hat{y}) \in \hat{T}^2, \end{cases} \tag{2.46}$$

which are continuous across the interface together with their fluxes. The coefficients $\hat{c}_k,\ k = 4, 5, 6$ are further determined by applying the extended jump conditions (2.11). Specifically, applying $(\mathbf{J}^t\hat{\nabla})$ leads to

$$(\mathbf{J}^t\hat{\nabla})\hat{\varphi}_k^{(2)}(\hat{x}, \hat{y}) = \begin{cases} (\mathbf{J}^t\hat{\nabla})\hat{\varphi}_i^{(1),1}\ \hat{\varphi}_j^{(1),1} + \hat{\varphi}_i^{(1),1}\ (\mathbf{J}^t\hat{\nabla})\hat{\varphi}_j^{(1),1} \\ +\frac{\hat{c}_k}{(1+a^2)}(\mathbf{J}^t\hat{\nabla})\left((\hat{y} - a\hat{x} - b)^2\right), \qquad (\hat{x}, \hat{y}) \in \hat{T}^1, \\ (\mathbf{J}^t\hat{\nabla})\hat{\varphi}_i^{(1),2}\ \hat{\varphi}_j^{(1),2} + \hat{\varphi}_i^{(1),2}\ (\mathbf{J}^t\hat{\nabla})\hat{\varphi}_j^{(1),2}\ , \qquad (\hat{x}, \hat{y}) \in \hat{T}^2, \end{cases}$$

which, in turn, yields

$$(\mathbf{J}^t\hat{\nabla})\cdot(\mathbf{J}^t\hat{\nabla})\hat{\varphi}_k^{(2)}(\hat{x},\hat{y}) = \begin{cases} 2\ (\mathbf{J}^t\hat{\nabla})\hat{\varphi}_i^{(1),1}\cdot(\mathbf{J}^t\hat{\nabla})\hat{\varphi}_j^{(1),1} \\ \qquad +\frac{\hat{c}_k}{(1+a^2)}\ (\mathbf{J}^t\hat{\nabla})\cdot(\mathbf{J}^t\hat{\nabla})\left((\hat{y}-a\hat{x}-b)^2\right)\ , & (\hat{x},\hat{y})\in\hat{T}^1, \\ 2\ (\mathbf{J}^t\hat{\nabla})\hat{\varphi}_i^{(1),2}\cdot(\mathbf{J}^t\hat{\nabla})\hat{\varphi}_j^{(1),2}\ , & (\hat{x},\hat{y})\in\hat{T}^2. \end{cases}$$

This can be written as

$$(\mathbf{J}^t\hat{\nabla})\cdot(\mathbf{J}^t\hat{\nabla})\hat{\varphi}_k^{(2)}(\hat{x},\hat{y}) = \begin{cases} 2\ (\mathbf{J}^t\hat{\nabla})\hat{\varphi}_i^{(1),1}\cdot(\mathbf{J}^t\hat{\nabla})\hat{\varphi}_j^{(1),1}+\frac{2\ \hat{c}_k}{(1+a^2)}(\mathbf{v}\cdot\mathbf{v})\ , & (\hat{x},\hat{y})\in\hat{T}^1, \\ 2\ (\mathbf{J}^t\hat{\nabla})\hat{\varphi}_i^{(1),2}\cdot(\mathbf{J}^t\hat{\nabla})\hat{\varphi}_j^{(1),2}\ , & (\hat{x},\hat{y})\in\hat{T}^2, \end{cases}$$

where $\mathbf{v}=(\mathbf{J}^t\hat{\nabla})(\hat{y}-a\hat{x}-b)$ is a constant vector. Applying the jump condition (2.11) yields

$$\hat{\beta}^1(\mathbf{J}^t\hat{\nabla})\hat{\varphi}_i^{(1),1}\cdot(\mathbf{J}^t\hat{\nabla})\hat{\varphi}_j^{(1),1}+\hat{\beta}^1\ ||\mathbf{v}||_2^2\ \frac{\hat{c}_k}{(1+a^2)}=\hat{\beta}^2\ (\mathbf{J}^t\hat{\nabla})\hat{\varphi}_i^{(1),2}\cdot(\mathbf{J}^t\hat{\nabla})\hat{\varphi}_j^{(1),2},$$

which, in turn, leads to

$$\hat{c}_k=-(1+a^2)\frac{[\hat{\beta}\ (\mathbf{J}^t\hat{\nabla}\hat{\varphi}_i^{(1)})\cdot(\mathbf{J}^t\hat{\nabla}\hat{\varphi}_j^{(1)})]_{\hat{\Gamma}}}{\hat{\beta}^1\ ||\mathbf{v}||_2^2}\ , \qquad k=4,5,6. \tag{2.47}$$

One can easily show that the six hierarchical shape functions $\hat{\varphi}_i^{(1)}, i=1,2,3$, $\hat{\varphi}_{3+i}^{(2)}, i=1,2,3$ constructed above form a basis of $\hat{\mathcal{R}}_1^2$.

The procedures above can be extended for constructing hierarchical shape functions for the IFE space $\hat{\mathcal{R}}_2^2(\hat{T})$.

3. Higher degree IFE spaces and shape functions

Now we consider immersed finite element spaces of arbitrary degree $p\geq 3$. We focus our discussion on the following IFE space:

(3.1)

$$\mathcal{R}_1^p(T)=\{U\ |\ U|_{T^\pm}\in\mathcal{P}_p,\ [U]_{T\cap\Gamma}=[\beta\frac{\partial U}{\partial\boldsymbol{n}}]_{T\cap\Gamma}=[\beta\frac{\partial^l\Delta U}{\partial\boldsymbol{n}^l}]_{T\cap\Gamma}=0, l=0,1,\ldots,p-2\},$$

which, on $\hat{T}$, becomes

(3.2)

$$\hat{\mathcal{R}}_1^p(\hat{T})=\{\hat{U}\in\hat{\mathcal{P}}_2(\hat{T}),|\ [\hat{U}]_{\hat{\Gamma}}=0,[\hat{\beta}\frac{\partial\hat{U}}{\partial\hat{\boldsymbol{n}}}]_{\hat{\Gamma}}=0,[\hat{\beta}\frac{\partial^l\hat{\Delta}\hat{U}}{\partial\hat{\boldsymbol{n}}^l}]_{\hat{\Gamma}}=0,\ l=0,1,\ldots,p-2\}.$$

Similar ideas can be applied to form $\mathcal{R}_2^p(T)$.

The Lagrange type shape functions can be constructed as follows. On each element $\hat{T}$ there are $ndim=dim(\mathcal{P}_p)$ nodes $\hat{V}_i,\ i=1,2,\ldots,ndim$ and the associated standard Lagrange shape functions $\hat{L}_i,\ i=1,2,\ldots,ndim$. Their indices are divided into $\mathscr{I}^1$, $\mathscr{I}^2$ and $\mathscr{I}^0$, respectively, which are the sets of indices for nodes in $\hat{T}^1$, $\hat{T}^2$ and on the interface $\hat{\Gamma}\cap\hat{T}$. Then, we define the Lagrange type IFE shape functions for $\hat{\mathcal{R}}_1^p$ as follows:

$$\hat{\varphi}_i(\hat{x},\hat{y})=\begin{cases}\hat{L}_i(\hat{x},\hat{y})+\sum\limits_{j\in\mathscr{I}^2}c_j\hat{L}_j(\hat{x},\hat{y}) & on\ \hat{T}^1,\\ \sum\limits_{j\in\mathscr{I}^1}c_j\hat{L}_j(\hat{x},\hat{y}) & on\ \hat{T}^2,\end{cases}\quad for\quad i\in\mathscr{I}^1, \tag{3.3a}$$

$$\hat{\varphi}_i(\hat{x},\hat{y})=\begin{cases}\sum\limits_{j\in\mathscr{I}^2}c_j\hat{L}_j(\hat{x},\hat{y}) & on\ \hat{T}^1\\ \hat{L}_i(\hat{x},\hat{y})+\sum\limits_{j\in\mathscr{I}^1}c_j\hat{L}_j(\hat{x},\hat{y}) & on\ \hat{T}^2\end{cases}\quad for\quad i\in\mathscr{I}^2, \tag{3.3b}$$

and

$$\hat{\varphi}_i(\hat{x},\hat{y}) = \begin{cases} \hat{L}_i(\hat{x},\hat{y}) + \sum\limits_{j\in\mathscr{I}^2} c_j \hat{L}_j(\hat{x},\hat{y}) & \text{on } \hat{T}^1 \\ \hat{L}_i(\hat{x},\hat{y}) + \sum\limits_{j\in\mathscr{I}^1} c_j \hat{L}_j(\hat{x},\hat{y}) & \text{on } \hat{T}^2 \end{cases} \quad for \quad i \in \mathscr{I}^0, \tag{3.3c}$$

where the coefficients $c_j,\ j = 1, 2, \ldots, |\mathscr{I}^1| + |\mathscr{I}^2|$ are determined by enforcing the jump conditions in (3.2) with suitable number of points on $\hat{\Gamma}$ according to the degree of the involved polynomials. These local shape functions can also be used to construct a Lagrange type p^{th} degree IFE spaces $\mathcal{S}_h^{p,1}$ and $\mathcal{S}_{h,0}^{p,1}$ over Ω through the standard procedure. We would like to mention that the procedure above can be easily adapted for constructing quadratic IFE shape functions.

Following [1, 27] and the reasoning for constructing quadratic hierarchical IFE spaces we construct p^{th} degree hierarchical IFE shape functions for $\hat{\mathcal{R}}_1^p,\ p \geq 3$. On non-interface elements use standard hierarchical bases [1, 27] while on each interface triangle we consider an IFE basis consisting of

- 3 vertex piecewise linear IFE shape functions

$$\hat{\varphi}_i^{(1)},\ i = 1, 2, 3, \tag{3.4}$$

- $3(p-1)$ edge IFE shape functions

(3.5)

$$\hat{\varphi}_i^{(k)} = \begin{cases} \hat{\varphi}_{3+i}^{(2),1}(\hat{\varphi}_i^{(1),1})^{k-2} + \sum\limits_{l=2}^{k} c_l(\hat{y} - a\hat{x} - b)^l, & \text{on } \hat{T}^1 \\ \hat{\varphi}_{3+i}^{(2),2}(\hat{\varphi}_i^{(1),2})^{k-2}, & \text{on } \hat{T}^2 \end{cases} \quad k = 2, 3, \ldots, p,\ i = 1, 2, 3,$$

where the superscript k denotes the polynomial degree and the subscript i denotes the edge number, and

- $(p-1)(p-2)/2$ (for $p \geq 3$) interior IFE shape functions

$$\hat{\varphi}_{i,j}^{(3+i+j)} = \begin{cases} \hat{\varphi}^{I,1}(\hat{\varphi}_1^{(1),1})^i(\hat{\varphi}_2^{(1),1})^j + \sum\limits_{l=2}^{3+i+j} c_l(\hat{y} - a\hat{x} - b)^l, & \text{on } \hat{T}^1 \\ \hat{\varphi}^{I,2}(\hat{\varphi}_1^{(1),2})^i(\hat{\varphi}_2^{(1),2})^j, & \text{on } \hat{T}^2 \end{cases} \tag{3.6}$$

with $0 \leq i + j \leq p - 3$, where

$$\hat{\varphi}^{I,k} = \hat{\varphi}_1^{(1),k}\hat{\varphi}_2^{(1),k}\hat{\varphi}_3^{(1),k},\ k = 1, 2. \tag{3.7}$$

One can easily verify that edge and interior shape functions and their fluxes are continuous across the interface. We determine the coefficients $c_2, c_3, \ldots$ to satisfy the extended interface conditions in $\hat{\mathcal{R}}_1^p$. We further note that interior IFE shape functions are supported on one element only.

4. Finite element methods for interface problems

In this section we present a finite element method for solving the interface problem (1.1) with the proposed higher degree IFE spaces. We assume that the true solution u belongs to the function space

$$\mathcal{S}(\Omega) = \{u,\ u|_{\Omega^\pm} \in H^{p+1}(\Omega^\pm),\ [u]_\Gamma = [\beta\ \boldsymbol{n}\cdot\nabla u]_\Gamma = 0\}. \tag{4.1}$$

Next we define a subset of the space $\mathcal{S}_h^{p,k}$ consisting of functions interpolating the essential boundary condition g

$$\mathcal{S}_{h,E}^{p,k} = \{U \in \mathcal{S}_h^{p,k} \,|\, U = \sum_{i=1}^{N_I} c_i \psi_i^{(k)} + \sum_{i=N_I+1}^{N} g(\mathbf{v}_i)\psi_i^{(k)}\}. \tag{4.2}$$

Let us recall the IFE method that exhibited optimal convergence rates for linear, bilinear and one-dimensional higher degree IFE spaces [3, 15, 20]: find $U^h \in \mathcal{S}_{h,E}^{p,k}$ such that

$$\sum_{T\in\mathcal{T}_h} \int_T \beta \nabla U^h \nabla V^h dxdy = \sum_{T\in\mathcal{T}_h} \int_T f V^h dxdy, \ \forall\ V^h \in \mathcal{S}_{h,0}^{p,k}. \tag{4.3}$$

However, our numerical experiments indicate that this IFE formulation does not converge optimally in $\mathcal{S}_{h,E}^{2,k}$. The IFE solution produced by this method has a large error across interface edges which, we believe, is caused by the discontinuity of the IFE functions. While this discontinuity does not prevent the method based on either linear or bilinear IFE functions to converge optimally, it becomes severe enough for higher degree IFE functions such that the method can only perform sub-optimally. To overcome this defect, we propose to employ penalization and stabilization in IFE methods. The idea is based on the Non-Symmetric Interior Penalty Galerkin (NIPG) method [10, 26] and our penalized IFE method described below follows from the standard Galerkin formulation plus penalties applied on interface edges only.

We now introduce a few notations and conventions in order to describe the formulation with interior penalty terms. Let $\mathcal{E}_h$, $\mathcal{E}_h^0$, $\mathcal{E}_h^i$ and $\mathcal{E}_h^{(0,i)}$ be the set of all the edges, interior edges, interface edges and interior interface edges in a mesh $\mathcal{T}_h$, respectively. For $e \in \mathcal{E}_h^0$ shared by two elements T_1 and T_2, let the vectors $\boldsymbol{n}_1$ and $\boldsymbol{n}_2$, respectively, be the unit vectors normal to e, pointing towards the exterior of T_1 and T_2. Following [23], for a scalar piecewise smooth function u, we let $u|_{T_i} = u_i,\ i = 1, 2$, and we will use the average and jump of u on an edge e defined by

$$\{u\} = \frac{1}{2}(u_1 + u_2) \qquad \text{and} \qquad [u] = u_1\mathbf{n_1} + u_2\mathbf{n_2}. \tag{4.4a}$$

Similarly for a vector-valued piecewise smooth function $\boldsymbol{\tau}$ such that $\boldsymbol{\tau}|_{T_i} = \boldsymbol{\tau}_i,\ i = 1, 2$ we define its average and jump by

$$\{\boldsymbol{\tau}\} = \frac{1}{2}(\boldsymbol{\tau}_1 + \boldsymbol{\tau}_2) \qquad \text{and} \qquad [\boldsymbol{\tau}] = \boldsymbol{\tau}_1 \cdot \mathbf{n_1} + \boldsymbol{\tau}_2 \cdot \mathbf{n_2}. \tag{4.4b}$$

We will also use the following notations

$$(u, v)_{\mathcal{T}_h} = \sum_{T\in\mathcal{T}_h} \int_T u\, v\ \ dxdy, \text{ and } < u, v >_{\mathcal{E}_h^t} = \sum_{e\in\mathcal{E}_h^t} \int_e u\, v\ \ ds, \tag{4.5}$$

for t being either $(0, i)$, or i. Then our partially penalized p^{th} degree IFE method is stated as: find $U^h \in \mathcal{S}_{h,E}^{p,k}, k = 1, 2$ such that

$$\begin{aligned}(\beta\nabla U^h, \nabla V^h)_{\mathcal{T}_h} + < [U^h], \{\beta\nabla V^h\} >_{\mathcal{E}_h^{0,i}} - < \{\beta\nabla U^h\}, [V^h] >_{\mathcal{E}_h^{0,i}} + \\ s < [U^h], [V^h] >_{\mathcal{E}_h^{0,i}} - \int_{\mathcal{E}_h^i\cap\partial\Omega} \beta\nabla U^h \cdot \boldsymbol{n}\ V^h\ ds = (f,\ V^h)_{\mathcal{T}_h}, \\ \forall\ V^h \in \mathcal{S}_{h,0}^{p,k}.\end{aligned} \tag{4.6}$$

We note that this scheme follows directly from the NIPG method [10, 26] with a minor modification that the penalization is partially applied only on interface edges where IFE functions are continuous. We have focused on the NIPG formulation for higher degree IFEs because of its flexibility about the choice of the penalty parameter s as suggested by the analysis for NIPG finite element in the literature. We experimented this scheme with various values for the penalty parameter s such as $s = 100, s = 1$ and $s = 0.01$ and we observed similar convergence behaviors; therefore, in the discussion from now on, we set $s = 1$ just for the simplicity. We believe that other formulations with partial penalty, such as those discussed in [29], can also be applied to higher degree IFEs, but those schemes usually require a suitable choice for the value of the penalization parameter. We plan to investigate related issues in a forthcoming article for extending higher degree IFEs to problems with general curve interfaces.

Finally, we note that fully discontinuous Galerkin finite element methods [16, 17, 24, 25] may be used to solve interface problems with the proposed p^{th} degree IFE spaces, but those methods will have more global degrees of freedom than the partially penalized IFE methods described above.

5. Computational examples

In this section we present numerical results for several interface problems to demonstrate the approximation capability of higher degree IFE spaces developed in the previous sections. All IFE spaces in these numerical experiments are constructed on uniform triangular meshes $\mathcal{T}_h$ that are formed by partitioning Ω into $(1/h)^2$ squares, then forming the triangular elements by joining the lower left and upper right vertices of these squares. Data presented in this section are generated with higher degree IFE spaces $S_h^{p,1}$. Results generated with IFE spaces $S_h^{p,2}$ have similar features; hence they are omitted here for the sake of reducing presentation space. In our numerical experiments, both IFE interpolations and IFE solutions generated by the partially penalized scheme to the second order elliptic interface problems converge optimally.

Example 5.1.

This example is to demonstrate the optimal approximation capability of the higher degree IFE spaces by the convergence rates of IFE interpolations of the following function:

(5.1)
$$\begin{cases} \frac{(6x^2+6xy-4x+3)\ \cos(y^2-x^2-\frac{4}{3}y+\frac{4}{9})+(2+3x-3y)\ \sin(\frac{2}{3}-x-y)}{3\beta^+}, & \text{on } \Omega^+, \\ \frac{(\frac{\beta^-}{\beta^+}-1)(3-8x+12xy)+(6x^2+6xy-4x+3)\ \cos(y^2-x^2-\frac{4}{3}y+\frac{4}{9})+(2+3x-3y)\ \sin(\frac{2}{3}-x-y)}{3\beta^-}, & \text{on } \Omega^-, \end{cases}$$

where the domain $\Omega = [0,1]^2$ is cut by the interface $\Gamma : y = x + \frac{2}{3}$ such that $\Omega^+ = \{(x,y), y > x + \frac{2}{3}\}$, $\Omega^- = \{(x,y), y < x + \frac{2}{3}\}$, and $r = \frac{\beta^+}{\beta^-}$ that represents a moderate discontinuity in the coefficient β when $r = 5$ or a large discontinuity when $r = 10^3$.

As usual, the Lagrange type IFE interpolant $I_h u(x,y)$ of $u(x,y)$ is defined by

$$I_h u(x,y)|_T = \sum_{i=1}^{(p+1)(p+2)/2} u(V_i)\phi_i^{(p)}(x,y),\ \forall\ T \in \mathcal{T}_h, \tag{5.2}$$

where $V_i,\ i = 1, 2, \ldots, (p+1)(p+2)/2$ are the Lagrange nodes for p^{th} degree polynomials in T and $\phi_i^{(p)}(x,y),\ i = 1, 2, \ldots, (p+1)(p+2)/2$ are the Lagrange FE

or IFE shape functions defined on T depending on whether T is a non-interface or an interface element.

Tables 5.1 and 5.2 present errors of $I_h u$ in both L^2 and semi-H^1 norms for the quadratic IFE space $S_h^{2,1}$. Errors of $I_h u \in S_h^{3,1}$ are given in Tables 5.3 and 5.4. Finally, errors of $I_h u \in S_h^{4,1}$ are given in Tables 5.5 and 5.6. All of these data indicate that IFE interpolants $I_h u \in S_h^{p,1}, p = 2, 3, 4$ converge to u optimally in both L^2 and H^1 norms regardless of a moderate or large discontinuity in β.

TABLE 5.1. L^2 interpolation errors and their orders for u, u_x and u_y for the function (5) with $r = 5$ using the IFE space $\mathcal{S}_h^{2,1}$.

h	$\|\|u - I_h u\|\|_0$	order	$\|\|u_x - (I_h u)_x\|\|_{0,h}$	order	$\|\|u_y - (I_h u)_y\|\|_{0,h}$	order
$\frac{1}{4}$	1.824818e-03	N/A	5.509363e-02	N/A	3.422630e-02	N/A
$\frac{1}{8}$	2.286751e-04	2.9963	1.383511e-02	1.9935	8.736473e-03	1.9699
$\frac{1}{16}$	2.857819e-05	3.0003	3.454655e-03	2.0017	2.189569e-03	1.9964
$\frac{1}{32}$	3.573301e-06	2.9995	8.640540e-04	1.9993	5.482050e-04	1.9978
$\frac{1}{64}$	4.465973e-07	3.0002	2.159648e-04	2.0003	1.370356e-04	2.0001
$\frac{1}{128}$	5.582714e-08	2.9999	5.399578e-05	1.9999	3.426435e-05	1.9998

TABLE 5.2. L^2 interpolation errors and their orders for u, u_x and u_y for the function (5) with $r = 10^3$ using the IFE space $\mathcal{S}_h^{2,1}$.

h	$\|\|u - I_h u\|\|_0$	order	$\|\|u_x - (I_h u)_x)\|\|_{0,h}$	order	$\|\|u_y - (I_h u)_y)\|\|_{0,h}$	order
$\frac{1}{4}$	1.825604e-03	N/A	5.512166e-02	N/A	3.428669e-02	N/A
$\frac{1}{8}$	2.307696e-04	2.9838	1.395794e-02	1.9815	8.880656e-03	1.9489
$\frac{1}{16}$	2.857665e-05	3.0135	3.454740e-03	2.0144	2.189942e-03	2.0197
$\frac{1}{32}$	3.579449e-06	2.9970	8.654861e-04	1.9969	5.499555e-04	1.9935
$\frac{1}{64}$	4.465694e-07	3.0027	2.159599e-04	2.0027	1.370315e-04	2.0048
$\frac{1}{128}$	5.584678e-08	2.9993	5.401489e-05	1.9993	3.428750e-05	1.9987

TABLE 5.3. Interpolation errors and their orders for the function (5) with $r = 5$ using the IFE space $\mathcal{S}_h^{3,1}$

h	$\|\|u - I_h u\|\|_0$	order	$\|\|u_x - (I_h u)_x)\|\|_{0,h}$	order	$\|\|u_y - (I_h u)_y)\|\|_{0,h}$	order
$\frac{1}{6}$	2.7113e-05	NA	1.5579e-03	NA	7.0126e-04	NA
$\frac{1}{12}$	1.6998e-06	3.9956	1.9537e-04	2.9953	8.8603e-05	2.9845
$\frac{1}{18}$	3.3603e-07	3.9980	5.7937e-05	2.9978	2.6306e-05	2.9950
$\frac{1}{24}$	1.0635e-07	3.9989	2.4450e-05	2.9989	1.1106e-05	2.9975
$\frac{1}{33}$	2.9760e-08	3.9994	9.4072e-06	2.9994	4.2739e-06	2.9986
$\frac{1}{42}$	1.1343e-08	3.9997	4.5634e-06	2.9996	2.0735e-06	2.9992
$\frac{1}{51}$	5.2174e-09	3.9998	2.5489e-06	2.9998	1.1582e-06	2.9995
$\frac{1}{63}$	2.2407e-09	3.9999	1.3522e-06	2.9998	6.1447e-07	2.9997

Example 5.2.

In this example, we first show that the non-conforming Galerkin scheme (4.3) does not converge when it is used with the quadratic IFE spaces even though

TABLE 5.4. Interpolation errors and their orders for the function (5) with $r = 10^3$ using the IFE space $\mathcal{S}_h^{3,1}$

h	$\|\|u - I_h u\|\|_0$	order	$\|\|u_x - (I_h u)_x)\|\|_{0,h}$	order	$\|\|u_y - (I_h u)_y)\|\|_{0,h}$	order
$\frac{1}{6}$	2.7111e-05	NA	1.5578e-03	NA	7.0105e-04	NA
$\frac{1}{12}$	1.6996e-06	3.9956	1.9536e-04	2.9953	8.8575e-05	2.9845
$\frac{1}{18}$	3.3600e-07	3.9980	5.7935e-05	2.9978	2.6298e-05	2.9950
$\frac{1}{24}$	1.0635e-07	3.9989	2.4449e-05	2.9989	1.1102e-05	2.9975
$\frac{1}{33}$	2.9757e-08	3.9994	9.4069e-06	2.9994	4.2726e-06	2.9986
$\frac{1}{42}$	1.1342e-08	3.9997	4.5633e-06	2.9996	2.0728e-06	2.9992
$\frac{1}{51}$	5.2170e-09	3.9998	2.5488e-06	2.9998	1.1578e-06	2.9995
$\frac{1}{63}$	2.2406e-09	3.9999	1.3522e-06	2.9998	6.1428e-07	2.9997

TABLE 5.5. Interpolation errors and their orders for the function (5) with $r = 5$ using the IFE space $\mathcal{S}_h^{4,1}$

h	$\|\|u - I_h u\|\|_0$	order	$\|\|u_x - (I_h u)_x)\|\|_{0,h}$	order	$\|\|u_y - (I_h u)_y)\|\|_{0,h}$	order
$\frac{1}{4}$	6.5831e-06	NA	3.5068e-04	NA	1.7890e-04	NA
$\frac{1}{8}$	2.2653e-07	4.8610	2.4260e-05	3.8535	1.1540e-05	3.9544
$\frac{1}{16}$	7.2422e-09	4.9671	1.5527e-06	3.9657	7.2846e-07	3.9857
$\frac{1}{32}$	2.2753e-10	4.9923	9.7591e-08	3.9919	4.5607e-08	3.9975
$\frac{1}{64}$	7.1207e-12	4.9979	6.1086e-09	3.9978	2.8525e-09	3.9989
$\frac{1}{128}$	2.2259e-13	4.9995	3.8191e-10	3.9995	1.7829e-10	4.0000

TABLE 5.6. Interpolation errors and their orders for the function (5) with $r = 10^3$ using the IFE space $\mathcal{S}_h^{4,1}$

h	$\|\|u - I_h u\|\|_0$	order	$\|\|u_x - (I_h u)_x)\|\|_{0,h}$	order	$\|\|u_y - (I_h u)_y)\|\|_{0,h}$	order
$\frac{1}{4}$	1.9895e-05	NA	1.1000e-03	NA	1.0567e-03	NA
$\frac{1}{8}$	5.0327e-07	5.3049	5.7995e-05	4.2454	5.3953e-05	4.2917
$\frac{1}{16}$	1.0195e-08	5.6253	2.2257e-06	4.7036	1.7516e-06	4.9449
$\frac{1}{32}$	2.9742e-10	5.0993	1.3265e-07	4.0685	1.0078e-07	4.1194
$\frac{1}{64}$	7.8165e-12	5.2498	6.7474e-09	4.2972	4.0416e-09	4.6402
$\frac{1}{128}$	2.4026e-13	5.0239	4.1792e-10	4.0130	2.4618e-10	4.0372

this scheme works optimally with the linear and bilinear IFE spaces. Then, we demonstrate that the partially penalized IFE method (4.6) can produce solutions to interface problems with optimal convergence rates.

First, we consider the interface problem (1.1) whose true solution is given in (5) where $\frac{\beta^+}{\beta^-} = 5$. Errors of quadratic IFE solutions produced by non-conforming Galerkin scheme (4.3) are reported in Table 5.7. Data in this table does not suggest any convergence pattern if any at all.

Next, we solve the same interface problem for $\frac{\beta^+}{\beta^-} = 5$ and $\frac{\beta^+}{\beta^-} = 10^3$ on the same meshes by the partially penalized IFE method (4.6) using quadratic IFE spaces $\mathcal{S}_h^{2,1}$. The errors and orders of convergence in these quadratic IFE solutions are presented in Tables 5.8, 5.9. From these results, we can easily observe that the partially penalized IFE method performs optimally with the quadratic IFE space $\mathcal{S}_h^{2,1}$ for interface problems with both a moderate and a large discontinuity in coefficients.

TABLE 5.7. L^2 errors and their orders for quadratic IFE solution U^h and its derivatives for Example 5.2 with $r = 5$ using the method (4.3) with $\mathcal{S}_h^{2,1}$.

h	$\|\|u - U^h\|\|_0$	order	$\|\|u_x - U_x^h\|\|_{0,h}$	order	$\|\|u_y - U_y^h\|\|_{0,h}$	order
$\frac{1}{4}$	1.895109e-03	N/A	5.541022e-02	N/A	3.524658e-02	N/A
$\frac{1}{8}$	4.842859e-04	1.9683	1.849617e-02	1.5829	1.451450e-02	1.2799
$\frac{1}{16}$	6.071277e-05	2.9957	4.626621e-03	1.9991	3.856017e-03	1.9123
$\frac{1}{32}$	5.041339e-05	0.2681	5.654537e-03	-0.2894	5.481738e-03	-0.5075
$\frac{1}{64}$	6.476201e-06	2.9605	1.545544e-03	1.8712	1.543935e-03	1.8280
$\frac{1}{128}$	6.674539e-06	-0.0435	2.706456e-03	-0.8082	2.683355e-03	-0.7974

TABLE 5.8. L^2 errors and their orders for quadratic IFE solution U^h and its derivatives for Example 5.2 with $r = 5$ using the partially penalized method with $\mathcal{S}_h^{2,1}$.

h	$\|\|u - U^h\|\|_0$	order	$\|\|u_x - U_x^h\|\|_{0,h}$	order	$\|\|u_y - U_y^h\|\|_{0,h}$	order
$\frac{1}{4}$	2.185943e-03	N/A	1.862205e-02	N/A	2.458501e-02	N/A
$\frac{1}{8}$	2.746045e-04	2.9928	4.496799e-03	2.0500	6.257552e-03	1.9741
$\frac{1}{16}$	3.426104e-05	3.0027	1.105460e-03	2.0242	1.565315e-03	1.9991
$\frac{1}{32}$	4.284828e-06	2.9992	2.757968e-04	2.0029	3.916519e-04	1.9988
$\frac{1}{64}$	5.355157e-07	3.0002	6.883339e-05	2.0024	9.787855e-05	2.0005
$\frac{1}{128}$	5.582693e-08	3.0001	5.399404e-05	1.9999	3.426510e-05	1.9998

TABLE 5.9. L^2 errors and their orders for quadratic IFE solution U^h and its derivatives for Example 5.2 with $r = 10^3$ using the partially penalized method with $\mathcal{S}_h^{2,1}$.

h	$\|\|u - U^h\|\|_0$	order	$\|\|u_x - U_x^h\|\|_{0,h}$	order	$\|\|u_y - U_y^h\|\|_{0,h}$	order
$\frac{1}{4}$	2.008170e-03	N/A	5.644459e-02	N/A	3.510983e-02	N/A
$\frac{1}{8}$	2.340102e-04	3.1012	1.383754e-02	2.0282	8.805326e-03	1.9954
$\frac{1}{16}$	2.891611e-05	3.0166	3.464429e-03	1.9978	2.199582e-03	2.0011
$\frac{1}{32}$	3.584640e-06	3.0119	8.641624e-04	2.0032	5.489480e-04	2.0024
$\frac{1}{64}$	4.473714e-07	3.0022	2.160397e-04	2.0000	1.371766e-04	2.0006
$\frac{1}{128}$	5.585713e-08	3.0017	5.399635e-05	2.0002	3.427253e-05	2.0010

Example 5.3.

There are many applications with great potentials to take advantage of the major strength of the IFE method which consists of its ability to be used on interface-independent meshes. For instance, let us consider the interface problem (1.1) on $\Omega = (0,1)^2$ consisting of two materials, one of them forms a thin layer in the top part of the domain. Specifically, we assume the interface is defined by

$$y = 1 - \epsilon,\ 0 < \epsilon < 1 \tag{5.3}$$

which separates Ω into $\Omega^+ = \{(x,y) \in \Omega, y > 1-\epsilon\}$ and $\Omega^- = \{(x,y) \in \Omega, y < 1-\epsilon\}$ as illustrated in Figure 5.1. The Dirichlet boundary condition and the source term

f are selected such that the true solution is

$$u(x,y) = \begin{cases} \frac{(1+x^3(y+e-1))\cos(x(y+e-1))+\sin(x(y+e-1))}{\beta^+}, & \text{on } \Omega^+, \\ \frac{(1+x^3(y+e-1))\cos(x(y+e-1))+\sin(x(y+e-1))-1}{\beta^-} + \frac{1}{\beta^+}, & \text{on } \Omega^-. \end{cases} \tag{5.4}$$

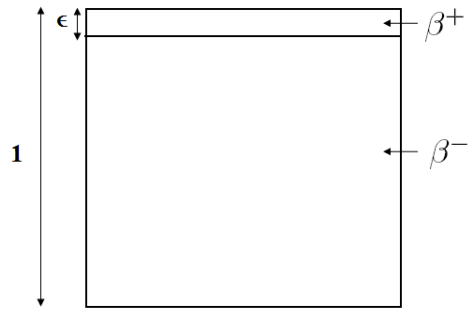

FIGURE 5.1. A two-material domain with a thin layer of width ϵ for Example 5.3.

We solve this problem for $\epsilon = 10^{-3}$ and $\frac{\beta^+}{\beta^-} = 5$ using the partially penalized IFE method (4.6) with the space $\mathcal{S}_h^{2,1}$ on uniform meshes. We present the L^2 errors for the quadratic IFE solution U^h and it derivatives in Table 5.10. For the sake of comparison, we also solve this problem using the standard quadratic finite element method with body-fitted meshes. The related computations are carried out through the software *COMSOL* using its default parameters except for "max element size" $hmax = 1/8, 1/16, 1/32$ and $1/64$. A typical mesh used in COMSOL for $hmax = 1/16$ and $\epsilon = 10^{-3}$ is shown in Figure 5.2.

We present errors in the finite element solution in Table 5.11 and plot the L^2 errors versus the number of degrees of freedom for both methods in Figure 5.3. From this simple experiment we observe that in order to produce numerical solutions with a comparable accuracy, the conventional finite element method with body-fitted meshes requires much more global degrees of freedom than the proposed partially penalized IFE method.

TABLE 5.10. Degrees of freedom (DOF) and errors in IFE solution $U^h \in S_h^{2,1}$ and its derivatives for Example 5.3 with $\epsilon = 10^{-3}$. The IFE solution U^h is produced by the proposed partially penalized IFE method on uniform meshes.

DOF	$\|\|u - U^h\|\|_0$	$\|\|u_x - U_x^h\|\|_{0,h}$	$\|\|u_y - U_y^h\|\|_{0,h}$
289	1.689638e-04	4.136825e-03	3.268165e-03
1089	2.137912e-05	1.041716e-03	8.173907e-04
4225	2.684222e-06	2.610211e-04	2.043138e-04
16641	3.362449e-07	6.529878e-05	5.107821e-05

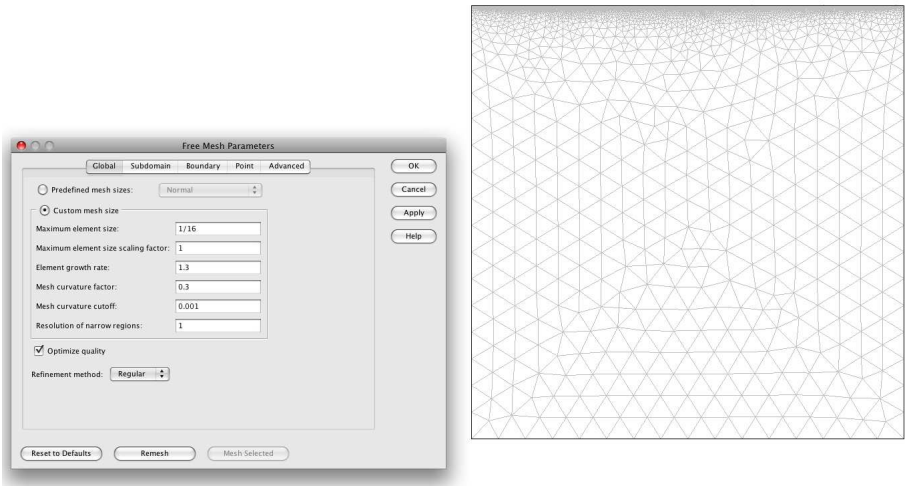

FIGURE 5.2. COMSOL-generated mesh for the two-material domain of Figure 5.1 with $\epsilon = 10^{-3}$.

TABLE 5.11. Degrees of freedom (DOF) and errors in FE solution U^h and its derivatives for Example 4 with $\epsilon = 10^{-3}$. The FE solution U^h is produced by the standard finite element method in COMSOL software on body-fitted meshes.

DOF	$\|\|u - U^h\|\|_0$	$\|\|u_x - U^h_x\|\|_{0,h}$	$\|\|u_y - U^h_y\|\|_{0,h}$
25550	1.838226e-04	5.894349e-03	4.736762e-03
25706	2.488306e-05	1.633209e-03	1.391346e-03
27182	3.049056e-06	4.049628e-04	3.783127e-04
32890	3.796342e-07	1.038044e-04	9.289677e-05

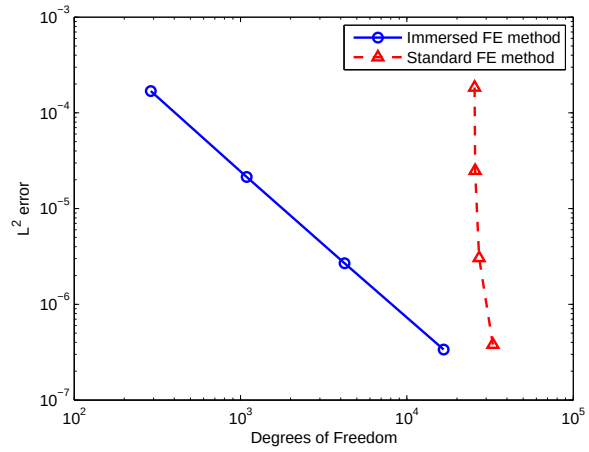

FIGURE 5.3. L^2 errors versus the number of degrees of freedom for immersed method on uniform meshes and for standard finite element method on body-fitted meshes using COMSOL for Example 5.3.

6. Conclusion

We have explored how to extend linear IFE functions to higher degree polynomials for solving the popular second order elliptic interface problems. Two classes of extended interface jump conditions are proposed for IFE functions with second degree polynomials and beyond on uniform triangular meshes. Procedures are developed for constructing higher degree IFE shape functions in both the Lagrange and hierarchical forms on interface elements. These higher degree IFE are numerically demonstrated to have the optimal approximation capability. A partially penalized IFE method is also developed to solve the second order elliptic interface problems with higher degree IFE spaces. Numerical results indicate that this partially penalized higher degree IFE method converges optimally and the penalization used in this scheme seems to be necessary for it to perform satisfactorily.

References

[1] S. Adjerid, M. Aiffa, and J.E. Flaherty. Hierarchical finite element bases for triangular and tetrahedral elements. *Computer Methods in Applied Mechanics and Engineering*, 190:2925–2941, 1999.

[2] S. Adjerid and T. Lin. Higher-order immersed discontinuous Galerkin methods. *International journal of information and systems sciences*, 3:558–565, 2007.

[3] S. Adjerid and T. Lin. A p^{th}-degree immersed finite element method for boundary value problems with discontinuous coefficients. *Applied Numerical Mathematics*, 59:1303–1321, 2009.

[4] I. Babuška and J. E. Osborn. Generalized finite element methods: their performance and relation to mixed methods. *SIAM J. Numer. Anal.*, 20(3):510–536, 1983.

[5] I. Babuška and J. E. Osborn. Finite element methods for the solution of problems with rough input data. In P. Grisvard, W. Wendland, and J.R. Whiteman, editors, *Singular and Constructive Methods for their Treatment, Lecture Notes in Mathematics, #1121*, pages 1–18, New York, 1985. Springer-Verlag.

[6] I. Babuška and J. E. Osborn. Can a finite element method perform arbitrarily badly? *Math. Comp.*, 69(230):443–462, 2000.

[7] M. Ben-Romdhane. *Higher-Degree Immersed Finite Elements for Second-Order Elliptic Interface Problems*. PhD thesis, Virginia Polytechnic Institute and State University, August 2011.

[8] D. Braess. *Finite Elements: Theory, Fast Solvers, and Applications in Solid Mechanics*. Cambridge University Press, New York, 2007.

[9] J. H. Bramble and J. T. King. A finite element method for interface problems in domains with smooth boundary and interfaces. *Adv. Comput. Math.*, 6:109–138, 1996.

[10] F. Brezzi, B. Cockburn, L.D. Marini, and E. Suli. Stabilization mechanisms in discontinuous Galerkin finite element methods. *Comput. methods in Appl. Mech. Engrg.*, 2005.

[11] B. Camp, T. Lin, Y. Lin, and W.-W. Sun. Quadratic immersed finite element spaces and their approximation capabilities. *Advances in Computational Mathematics*, 24:81–112, 2006.

[12] Z. Chen and J. Zou. Finite element methods and their convergence for elliptic and parabolic interface problems. *Numer. Math.*, 79:175–202, 1998.

[13] R.W. Clough and J.L. Tocher. Finite element stiffness matrices for analysis of plates in bending. In *Matrix Methods in Structual Mechanics, The Proceedings of the Conference held at Wright-Parrterson Air Force Base, Ohio, 26-28, October, 1965, edited by J.R. Prezemieniecki et al*, pages 515–545. National Technical Information Service, U.S. Department of Commerce, Virginia, 1966.

[14] Y. Gong, B. Li, and Z. Li. Immersed-interface finite-element methods for elliptic interface problems with non-homogeneous jump conditions. *SIAM J. Numer. Anal.*, 46:472–495, 2008.

[15] X. He, T. Lin, and Y. Lin. Approximation capability of a bilinear immersed finite element space. *Numerical Methods for Partial Differential Equations*, 24:1265–1300, 2008.

[16] X. He, T. Lin, and Y. Lin. Interior penalty bilinear IFE discontinuous Galerkin methods for elliptic equations with discontinuous coefficient. *Journal of Systems Science and Complexity*, 23:467-483, 2010.

[17] X. He, T. Lin, and Y. Lin. A selective immersed discontinuous Galerkin method for elliptic interface problems. *Mathematical Methods in the Applied Sciences*, 2013 (to appear).

[18] R. Kafafy, T. Lin, Y. Lin, and J. Wang. 3-D immersed finite element methods for electric field simulation in composite materials. *International Journal for Numerical Methods in Engineering*, 64:904–972, 2005.
[19] Z. Li. The immersed interface method using a finite element formulation. *Applied Numer. Math.*, 27:253–267, 1998.
[20] Z. Li, T. Lin, and X. Wu. New Cartesian grid methods for interface problems using finite element formulation. *Numerische Mathematik*, 96(1):61–98, 2003.
[21] Z. Li, T. Lin, Y. Lin, and R. Rogers. An immersed finite element space and its approximation capability. *Numerical Methods for Partial Differential Equations*, 20(3):338–367, 2004.
[22] T. Lin, Y. Lin, R. C. Rogers, and L. M. Ryan. A rectangular immersed finite element method for interface problems. In P. Minev and Y. Lin, editors, *Advances in Computation: Theory and Practice, Vol. 7*, pages 107–114. Nova Science Publishers, Inc., 2001.
[23] LD. Marini D.N. Arnold F. Brezzi, B. Cockburn. Unified analysis of discontinuous galerkin methods for elliptic problems. *SIAM J. Numer. Anal.*, 39:1749–1779, 2000.
[24] J.T. Oden, Ivo Babuska, and C.E. Baumann. A discontinuous hp finite element method for diffusion problems. *J. Comput. Phys.*, 146:491–519, 1998.
[25] Beatrice Rivière. *Discontinuous Galerkin Methods for Solving Elliptic and Parabolic Equations*. Frontiers in Applied Mathematics, FR35, SIAM, Philadelphia, 2008.
[26] B. Rivière, M.F. Wheeler, and V. Giraut. Improved energy estimates for finite elements methods based on discontinuous approximations spaces for elliptic problems. *SIAM Journal on Numerical Analysis*, 39:902–931, 2001.
[27] B. Szabo and I. Babuska. *Finite Element Analysis*. John Wiley, New York, 1991.
[28] Sylvain Vallaghé and Théodore Papadopoulo, A trilinear immersed finite element method for solving the electroencephalography forward problem. *SIAM J. Sci. Comput.*, 32:2379-2394, 2010.
[29] Xu Zhang. *Nonconforming Immersed Finite Element Methods for Interface Problems*. PhD thesis, Virginia Polytechnic Institute and State University, April 2013.

Department of Mathematics, Virginia Tech, Blacksburg, VA 24061, USA
E-mail: adjerids@math.vt.edu

Department of Mathematics and Natural Sciences, Gulf University for Science and Technology, P.O. Box: 7207 Hawally, 32093 Kuwait
E-mail: romdhane.m@gust.edu.kw

Department of Mathematics, Virginia Tech, Blacksburg, VA 24061, USA
E-mail: tlin@vt.edu